

REPORT DOCUMENTATION PAGEForm Approved
OMB No. 0704-0188

Public reporting burden for this collection of information is estimated to average 1 hour per response, including the time for reviewing instructions, searching existing data sources, gathering and maintaining the data needed, and completing and reviewing this collection of information. Send comments regarding this burden estimate or any other aspect of this collection of information, including suggestions for reducing this burden to Department of Defense, Washington Headquarters Services, Directorate for Information Operations and Reports (0704-0188), 1215 Jefferson Davis Highway, Suite 1204, Arlington, VA 22202-4302. Respondents should be aware that notwithstanding any other provision of law, no person shall be subject to any penalty for failing to comply with a collection of information if it does not display a currently valid OMB control number. **PLEASE DO NOT RETURN YOUR FORM TO THE ABOVE ADDRESS.**

1. REPORT DATE (DD-MM-YYYY) 14-03-1973		2. REPORT TYPE Interim Report		3. DATES COVERED (From - To) 01-01-1973 to 01-03-1973	
4. TITLE AND SUBTITLE Prediction of Transients in Buried, Shielded Cables				5a. CONTRACT NUMBER DAEA18-71-A-0204/D.O. 0006	
				5b. GRANT NUMBER	
				5c. PROGRAM ELEMENT NUMBER	
6. AUTHOR(S) Edward F. Vance				5d. PROJECT NUMBER 2192	
				5e. TASK NUMBER	
				5f. WORK UNIT NUMBER	
7. PERFORMING ORGANIZATION NAME(S) AND ADDRESS(ES) SRI International formerly Stanford Research Institute 333 Ravenswood Avenue Menlo Park, CA 94025				8. PERFORMING ORGANIZATION REPORT NUMBER L-29877	
9. SPONSORING / MONITORING AGENCY NAME(S) AND ADDRESS(ES) Procurement Division Headquarters Fort Huachuca P.O. Box 748 Fort Huachuca, AZ 85613				10. SPONSOR/MONITOR'S ACRONYM(S)	
				11. SPONSOR/MONITOR'S REPORT NUMBER(S)	
12. DISTRIBUTION / AVAILABILITY STATEMENT Approved for public release. Distribution is unlimited.					
13. SUPPLEMENTARY NOTES					
14. ABSTRACT This report contains simple formulas and graphs that can be used to obtain quick estimates of the total current induced in a buried cable by an incident plane-wave exponential pulse. Formulas and graphs are also given for estimating the internal voltage and current in cables with tubular shields when the total current in the cable is an exponential pulse, and when the current is induced in the cable by the incident exponential pulse.					
20040602 118					
15. SUBJECT TERMS					
16. SECURITY CLASSIFICATION OF:			17. LIMITATION OF ABSTRACT	18. NUMBER OF PAGES 86	19a. NAME OF RESPONSIBLE PERSON Margaret Baxter-Pearson
a. REPORT Unclassified	b. ABSTRACT Unclassified	c. THIS PAGE Unclassified			19b. TELEPHONE NUMBER (include area code) 650-859-4424

UNCLASSIFIED

Security Classification

DOCUMENT CONTROL DATA - R & D

(Security classification of title, body of abstract and indexing annotation must be entered when the overall report is classified)

1. ORIGINATING ACTIVITY (Corporate author) Stanford Research Institute Menlo Park, California 94306		2a. REPORT SECURITY CLASSIFICATION UNCLASSIFIED	
		2b. GROUP N/A	
3. REPORT TITLE PREDICTION OF TRANSIENTS IN BURIED, SHIELDED CABLES			
4. DESCRIPTIVE NOTES (Type of report and inclusive dates) Interim Technical Report Covering the period 1 January to 1 March 1973			
5. AUTHOR(S) (First name, middle initial, last name) Edward F. Vance			
6. REPORT DATE 14 March 1973		7a. TOTAL NO. OF PAGES 86	7b. NO. OF REFS
8a. CONTRACT OR GRANT NO. Contract DAEA18-71-A-0204		9a. ORIGINATOR'S REPORT NUMBER(S) Interim Technical Report SRI Project 2192	
b. PROJECT NO. Delivery Order 0006		9b. OTHER REPORT NO(S) (Any other numbers that may be assigned this report)	
c.			
d.			
10. DISTRIBUTION STATEMENT			
11. SUPPLEMENTARY NOTES		12. SPONSORING MILITARY ACTIVITY Procurement Division Headquarters Fort Huachuca (PROV) P.O. Box 748 Fort Huachuca, Arizona 85613	
13. ABSTRACT This report contains simple formulas and graphs that can be used to obtain quick estimates of the total current induced in a buried cable by an incident plane-wave exponential pulse. Formulas and graphs are also given for estimating the internal voltage and current in cables with tubular shields when the total current in the cable is an exponential pulse, and when the current is that induced in the cable by the incident exponential pulse.			

14	KEY WORDS	LINK A		LINK B		LINK C	
		ROLE	WT	ROLE	WT	ROLE	WT
	Buried cables Shielded cables Induced currents						
13. ABSTRACT (Continued)							



STANFORD RESEARCH INSTITUTE
Menlo Park, California 94025 · U.S.A.

Interim Technical Report

14 March 1973

PREDICTION OF TRANSIENTS IN BURIED, SHIELDED CABLES

By: E. F. VANCE

Prepared for:

PROCUREMENT DIVISION
HEADQUARTERS FORT HUACHUCA (PROV)
P.O. BOX 748
FORT HUACHUCA, ARIZONA 85613

Submitted in accordance with Item A007 of the Contract Data Requirements List.

CONTRACT DAEA18-71-A-0204

Delivery Order 0006
SRI Project 2192-NS

Approved by:

T. MORITA, *Director*
Electromagnetic Sciences Laboratory

RAY L. LEADABRAND, *Executive Director*
Electronics and Radio Sciences Division

Copy No.4

ABSTRACT

This report contains simple formulas and graphs that can be used to obtain quick estimates of the total current induced in a buried cable by an incident plane-wave exponential pulse. Formulas and graphs are also given for estimating the internal voltage and current in cables with tubular shields when the total current in the cable is an exponential pulse, and when the current is that induced in the cable by the incident exponential pulse.

CONTENTS

ABSTRACT iii

LIST OF ILLUSTRATIONS vii

I INTRODUCTION 1

II BULK CURRENT IN BURIED CABLES 3

 A. General 3

 B. Current Far from the Ends of a Long Cable 8

 1. Class of Problems 8

 2. Response Characteristics 8

 3. Theoretical Basis 13

 C. Current Near the End of a Long Bare Cable 18

 1. Class of Problems 18

 2. Response Characteristics 19

 3. Theoretical Basis 20

III CURRENTS AND VOLTAGES INDUCED ON INTERNAL CONDUCTORS 25

 A. General 25

 B. Electrically Short Cable with Tubular Shield
 (Cable Current Given) 25

 1. Class of Problems 25

 2. Response Characteristics 28

 3. Theoretical Basis 33

 C. Correction Factor for Long Cables 36

 1. Class of Problems 36

 2. Response Characteristics 37

 3. Theoretical Basis 39

 D. Internal Voltage from Incident Field 45

 1. Class of Problems 45

 2. Response Characteristics 45

 3. Theoretical Basis 46

E. Multiple Shields	48
1. Class of Problems	48
2. Equivalent Shield Characteristics	48
3. Theoretical Basis	49
Appendix A LIST OF SYMBOLS	53
Appendix B TRANSMISSION-LINE FORMULAS	57
Appendix C CHARACTERISTIC IMPEDANCE OF TRANSMISSION-LINE CONFIGURATIONS	61
Appendix D CONDUCTIVITY AND RELATIVE PERMEABILITY OF SHIELDING MATERIALS	65
Appendix E WIRE TABLE	69
Appendix F GROUND CONDUCTIVITY IN THE UNITED STATES	73

ILLUSTRATIONS

1	Illustration of Coordinates for Cable and Angle of Arrival of Transient Wave	3
2	Skin Depth δ in Soil as a Function of Frequency and Soil Conductivity σ	4
3	Waveforms of Incident Exponential Pulse and Cable Currents	10
4	Variation of Peak Cable Current as Azimuth (φ) and Elevation (ψ) Angles of Incidence Change $[D(\psi, \varphi)]$	11
5	Peak Cable Current as a Function of Soil Conductivity and Incident Exponential Pulse-Decay Time Constant τ $[D(\psi, \varphi) = 1]$	12
6	Variation of Log $(\sqrt{2}\delta/\gamma_0 a)$ with Frequency and Conductor Radius. (Note that a factor of 10 in conductor radius produces the same effect as a factor of 100 in soil conductivity.)	14
7	Variation of L/L_S and $R/w(L + L_S)$ with δ/a for an Insulated Buried Cable. (L is the inductance of the insulation gap, L_S is the inductance of the soil, and R is the soil resistance, all on a per-unit-length basis.)	18
8	Waveform of Cable Current Near the End when Sheath is Open-Circuit	21
9	Frequency at Which the Shield Wall Thickness T is one Skin Depth for Various Metals	26
10	The Diffusion Constant τ_s as a Function of Wall Thickness for Common Shielding Materials	27
11	Core Current Waveforms Produced by an Exponential Pulse $I_{SO}e^{-t/\tau}$ of Current in the Shield (normalized to $V_O/Z_O = I_{SO}R_O\ell/2Z_O$)	30
12	Open-Circuit Voltage $V_O = I_{SO}R_O\ell/2$ Between Core and Shield for Common Shielding Materials, Thicknesses, and Diameters (for $I_{SO} = 1$ ampere and $\ell = 1$ kilometer)	31

13	Variation of Peak Open-Circuit Voltage and Rise Time of Core-to-Shield Voltage as a Function of Exponential Shield-Current-Decay Time Constant τ (normalized to diffusion constant τ_s)	32
14	Correction Factor for the Peak Voltage and Current Induced in Long Shielded Cables (k' is the propagation factor for the shield current, $k = \omega\sqrt{\mu_0\epsilon_0}$, and ϵ_r is the dielectric constant of the core-to-shield insulation)	38
15	Core-Current Waveforms for Electrically Long Cables with an Exponential Shield Current $I_{s0}e^{-t/\tau}$. (τ_s is the shield diffusion constant, $\tau_r = 0.236 \tau_s$, and $l/v = l\sqrt{\epsilon_r}/c$ is the one-way transit time along the core.)	40
16	Differential Transit Time t_0 as a Function of Cable Length and Propagation Factor k' for the Shield Current for Polyethylene-Insulated Cable Core	41
17	Core-to-Shield Voltage Waveforms Induced in Buried Cable by an Incident Plane-Wave Exponential Pulse $e^{-t/\tau}$	47

38 This report has been prepared to assist the worker in EMP coupling
studies in obtaining quick estimates of the current induced in buried
cables and of the internal current and voltage induced in shielded
cables. An attempt has been made to organize the material in a format
40 that permits the desired result to be obtained with a minimum of addi-
tional calculation and without extraneous development of the theory
involved. Following the presentation of the results, however, a brief
41 explanation of their source is provided to give the interested reader
more insight into the nature and quality of the results. It is felt
that such information will be useful to the user in establishing the
47 applicability and limitations of the results, although the range of
applicability is summarized at the outset in each case under the heading
"Class of Problems."

The bulk (total) current in the buried cable is presented for a
plane-wave incident on the surface of the earth. The incident waveform
is an exponential pulse; however, the decay time constant is arbitrary
(within limits), so that incident field waveforms approaching an impulse
(very short decay) or a step function (very long decay) can be obtained.
The other parameters that affect the cable response are the direction
of arrival and the soil conductivity. The direction of arrival is a
geometric function that is a separable directivity coefficient $D(\psi, \varphi)$
of the current spectrum or waveform. The soil conductivity is incorpo-
rated through a soil time constant, $\tau_e = \epsilon_o / \sigma$, for convenient normaliza-
tion of the cable responses. Thus the bulk current in the cable is
defined in terms of the three parameters, τ (the incident-pulse decay

time constant), τ_e (the soil time constant), and $D(\psi, \varphi)$ (the directivity function), in addition to the amplitude of the incident field. A single waveform in normalized time t/τ describes the bulk current in a long buried cable.

The bulk current results are given only for the case in which the ground behaves as a conductor. For most angles of incidence and soil conductivities, this limitation is inconsequential for the EMP spectrum because the relative magnitude of the high-frequency spectrum where the soil behaves as a lossy dielectric is small and the attenuation of the field for typical cable burial depths at these frequencies is significant. Furthermore, the cable shield usually attenuates these frequencies so severely that they are completely negligible in the internal-voltage and -current analysis.

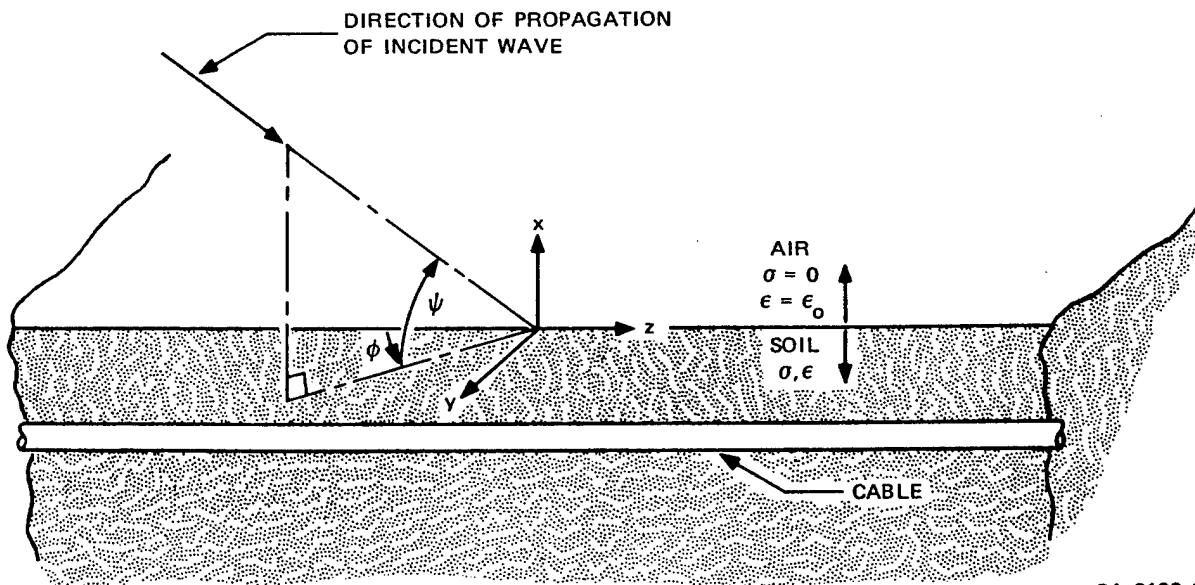
The internal voltage and current are presented for cables with uniform tubular shields. The important cable parameters affecting these internal responses are the dc resistance per unit length of the shield, the length of the cable, the shield diffusion time constant $\tau_s = \mu\sigma T^2$, and, for the core current, the characteristic impedance of the core-to-shield transmission line ("core" is used to designate all the conductors covered by the shield). The internal responses are presented for an exponential pulse of current in the shield. In addition, for electrically short cables the internal responses of a buried cable to an incident plane-wave exponential pulse are presented. Only open-circuit or matched (characteristic impedance) terminations are used for the internal responses presented here.

Finally, in an effort to make this document a more useful reference for the cable-coupling analyst, appendices containing transmission-line relations, electromagnetic properties of common shielding materials, a wire table, and a soil-conductivity map have been included. Appendix A is a list of the symbols used, and their meanings.

II BULK CURRENTS IN BURIED CABLES

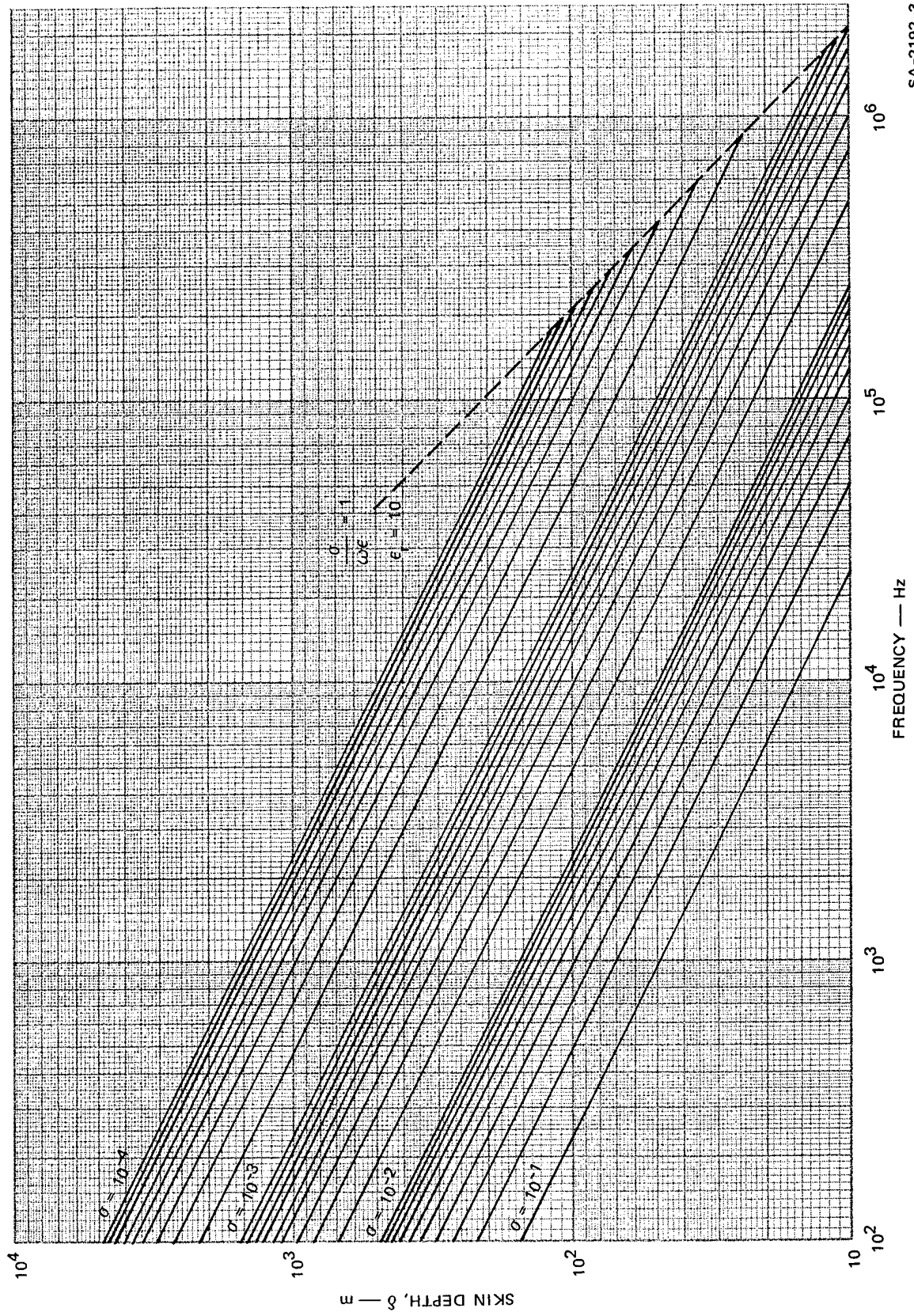
A. General

This section presents formulas for calculating the total current induced in a buried cable by an incident uniform plane wave, for bare and thinly insulated cables. The incident electromagnetic pulse is assumed to have an exponential waveform $E_0 \exp(-t/\tau)$. The wave is assumed to arrive on the surface of the earth from a direction defined by an elevation angle ψ and an azimuth angle ϕ as illustrated in Figure 1. The depth of burial of the cable is small compared to a skin depth in the soil, so that the fields at the cable depth are essentially the same as those at the surface.



SA-2192-2

FIGURE 1 ILLUSTRATION OF COORDINATES FOR CABLE AND ANGLE OF ARRIVAL OF TRANSIENT WAVE



SA-2192-3

FIGURE 2 SKIN DEPTH δ IN SOIL AS A FUNCTION OF FREQUENCY AND SOIL CONDUCTIVITY σ

In all the bulk-current formulas, the soil is considered to be a good conductor, as defined by $\sigma \gg \omega\epsilon$. The wave-propagation factor in the soil, and the propagation factor for bare conductors, is thus

$$\gamma = \sqrt{j\omega\mu_0(\sigma + j\omega\epsilon)} \approx \sqrt{j\omega\mu_0\sigma} = \frac{1+j}{\delta} \quad (1)$$

where δ is the skin depth in the soil. A plot of skin depth as a function of frequency and soil conductivity is given in Figure 2. The dashed line along the right-hand side of Figure 2 indicates the limit of validity of the approximation $\gamma \approx (1+j)/\delta$. Although this limit falls between a few hundred kHz and a few MHz for typical soil conductivities, most cable shields have very large attenuation at frequencies above 100 kHz, so that the bulk-current spectrum at these frequencies is usually of secondary interest.

The current induced in a buried cable is computed by treating the cable as a transmission line that is driven by the component of the underground electric field that is parallel to the axis of the cable. As illustrated in Figure 1, the z axis is parallel to the axis of the cable, and the direction of arrival of the incident wave will be specified by the elevation angle ψ and the azimuth angle φ . The phase of the incident wavefront at the air/earth interface is of the form $k \cos \psi \cos \varphi$, where $k = \omega\sqrt{\mu_0\epsilon_0}$, and the component of the electric field parallel to the cable will be

$$E_z = E(\omega)e^{-jk'z}(1 + R_h) \sin \varphi \quad (2)$$

for horizontal polarization, and

$$E_z = E(\omega)e^{-jk'z}(1 - R_v) \cos \varphi \sin \psi \quad (3)$$

for vertical polarization, where

$$k' = k \cos \psi \cos \varphi$$

$E(\omega)$ = Incident field strength

R_h = Reflection coefficient for the air/earth interface when the incident wave is horizontally polarized

R_v = Reflection factor when the incident wave is vertically polarized.

These reflection factors are given by

$$R_h = \frac{\sin \psi - \sqrt{\epsilon_r \left(1 + \frac{\sigma}{j\omega\epsilon}\right) - \cos^2 \psi}}{\sin \psi + \sqrt{\epsilon_r \left(1 + \frac{\sigma}{j\omega\epsilon}\right) - \cos^2 \psi}} \quad (4)$$

and

$$R_v = \frac{\epsilon_r \left(1 + \frac{\sigma}{j\omega\epsilon}\right) \sin \psi - \sqrt{\epsilon_r \left(1 + \frac{\sigma}{j\omega\epsilon}\right) - \cos^2 \psi}}{\epsilon_r \left(1 + \frac{\sigma}{j\omega\epsilon}\right) \sin \psi + \sqrt{\epsilon_r \left(1 + \frac{\sigma}{j\omega\epsilon}\right) - \cos^2 \psi}} \quad (5)$$

where σ is the soil conductivity, ϵ_r is the dielectric constant of the soil, and $\epsilon = \epsilon_0 \epsilon_r$. For $\sigma \gg \omega\epsilon$, the terms $(1 \pm R)$ reduce to

$$1 + R_h \approx \frac{2 \sin \psi}{\sqrt{\frac{\sigma}{j\omega\epsilon_0}}} \quad (6)$$

$$1 - R_v \approx \frac{2}{\sqrt{\frac{\sigma}{j\omega\epsilon_0}} \sin \psi} \quad (7)$$

The current induced in the cable is then

$$I(z, \omega) = [K_1 + P(z)]e^{-\gamma z} + [K_2 + Q(z)]e^{\gamma z} \quad (8)$$

where $\gamma = \sqrt{ZY}$, the propagation factor for the cable, with the soil as the return conductor. K_1 and K_2 are constants given by

$$K_1 = \rho_1 e^{\gamma z_1} \frac{\rho_2 P(z_2) e^{-\gamma z_2} - Q(z_1) e^{\gamma z_2}}{e^{\gamma(z_2 - z_1)} - \rho_1 \rho_2 e^{-\gamma(z_2 - z_1)}} \quad (9)$$

$$K_2 = \rho_2 e^{-\gamma z_2} \frac{\rho_1 Q(z_1) e^{\gamma z_1} - P(z_2) e^{-\gamma z_1}}{e^{\gamma(z_2 - z_1)} - \rho_1 \rho_2 e^{-\gamma(z_2 - z_1)}} \quad (10)$$

in which the reflection coefficients ρ_1 and ρ_2 are given by

$$\rho_1 = \frac{Z_1 - Z_0}{Z_1 + Z_0}, \quad \rho_2 = \frac{Z_2 - Z_0}{Z_2 + Z_0}, \quad (11)$$

and the source functions $P(z)$ and $Q(z)$ are

$$P(z) = \frac{1}{2Z_0} \int_{z_1}^z e^{\gamma v} E_z(v) dv \quad (12)$$

$$Q(z) = \frac{1}{2Z_0} \int_z^{z_2} e^{-\gamma v} E_z(v) dv \quad (13)$$

The impedances Z_1 and Z_2 are those that terminate the cable shield at the ends z_1 and z_2 , respectively. When $Z_1 = Z_2 = Z_0$, the values of ρ_1 , ρ_2 , K_1 , and K_2 are all zero. This is the case of infinitely long cables or cable shields terminated in their characteristic impedances.

The characteristic impedance Z_0 is obtained from the impedance per unit length, Z , and the admittance per unit length, Y , from $Z_0 = \sqrt{Z/Y}$.

B. Current Far From the Ends of a Long Cable

1. Class of Problems

The response characteristics presented here apply to points far (several soil skin depths) from the ends of long buried cables that have no insulation (or have insulation that is thin compared to the cable radius) over the sheath (shield or armor). These response characteristics also apply to cables with semiconducting jackets so that the metal sheath is effectively in contact with the soil. The responses are based on the assumption that the soil behaves as a conductor ($\sigma > \omega\epsilon$), and that the radius of the cable is small compared to a skin depth in the soil ($a \ll \delta$). The results are presented for an incident exponential pulse that propagates as a plane wave that is uniform (constant magnitude) over several soil skin depths along the cable. The skin depth δ in the soil is plotted in Figure 2 as a function of soil conductivity and frequency. The decay time constant τ of the exponential pulse is large compared to the soil time constant $\tau_e = \epsilon/\sigma$. The small resistance of the cable is neglected, and it is assumed that the depth of burial is small compared to the soil skin depth at the highest frequencies of interest.

2. Response Characteristics

The total current induced far from the ends of a long cable by an incident field $E_0 e^{-t/\tau}$ is given by

$$I(\omega) \approx I_0 \frac{1}{\sqrt{j\omega\tau} (j\omega + 1/\tau)} \quad (14)$$

in the frequency domain, or

$$i(t) = I_o e^{-t/\tau} \frac{2}{\sqrt{\pi}} \int_0^{\sqrt{t/\tau}} e^{-u^2} du \quad (15)$$

in the time domain, where

$$I_o \approx 10^6 \sqrt{\tau_e \tau} E_o D(\psi, \varphi) \quad (\text{amperes})$$

$$\tau_e = \frac{\epsilon_o}{\sigma} = \frac{8.85 \times 10^{-12}}{\sigma} = \text{Time constant of soil (seconds)}$$

τ = Decay time constant of incident pulse (seconds)

E_o = Peak electric-field strength of incident pulse (v/m)

$D(\psi, \varphi) = \cos \varphi$ for vertically polarized wave

= $\sin \psi \sin \varphi$ for horizontally polarized wave.

The waveform for $i(t)$ and the incident exponential pulse are shown in Figure 3 as a function of time in incident-pulse decay time constant.

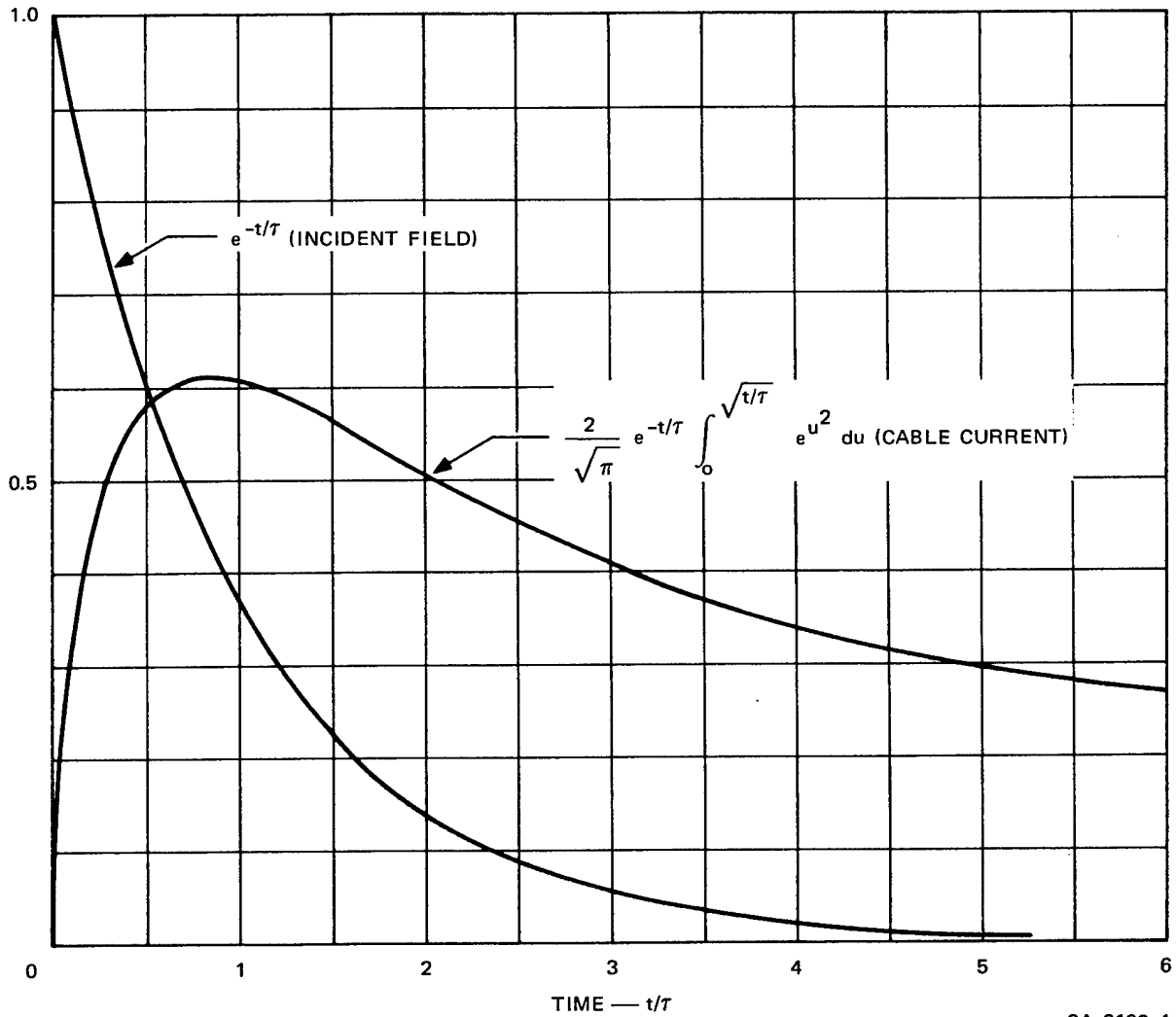
The peak current induced in the cable is

$$I_{pk} = I_o \left[e^{-t/\tau} \frac{2}{\sqrt{\pi}} \int_0^{\sqrt{t/\tau}} e^{-u^2} du \right]_{\max} = 0.61 I_o \quad (16)$$

and the peak current occurs at

$$t_{pk} = 0.85 \tau \quad (17)$$

The variation of the peak current with azimuth angle of incidence φ and elevation angle of incidence ψ is shown in Figure 4. The magnitude of the peak current for maximum coupling [$D(\psi, \varphi) = 1$] is plotted in Figure 5 as a function of soil conductivity for various incident-field time constants. The plots for constant τ are truncated in the lower left-hand

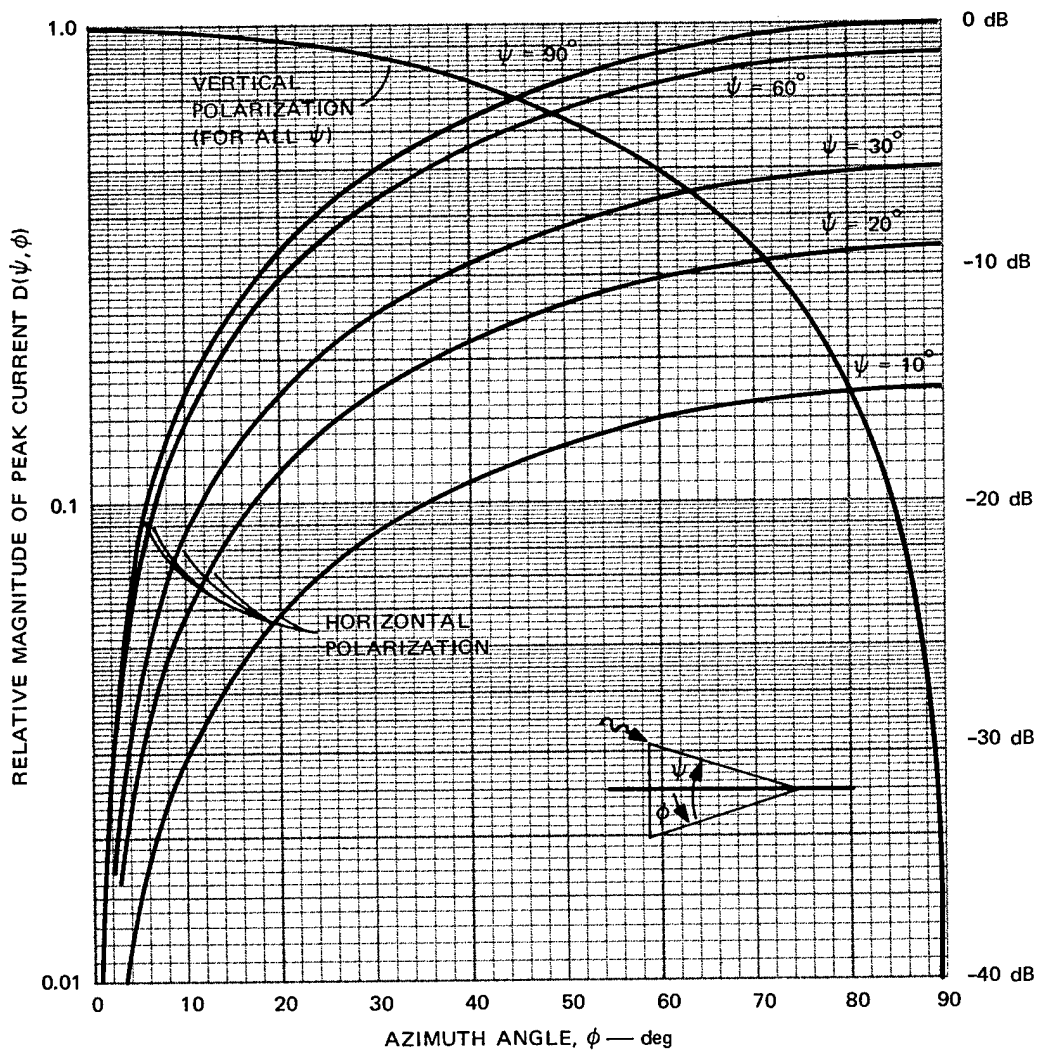


SA-2192-4

FIGURE 3 WAVEFORMS OF INCIDENT EXPONENTIAL PULSE AND CABLE CURRENTS

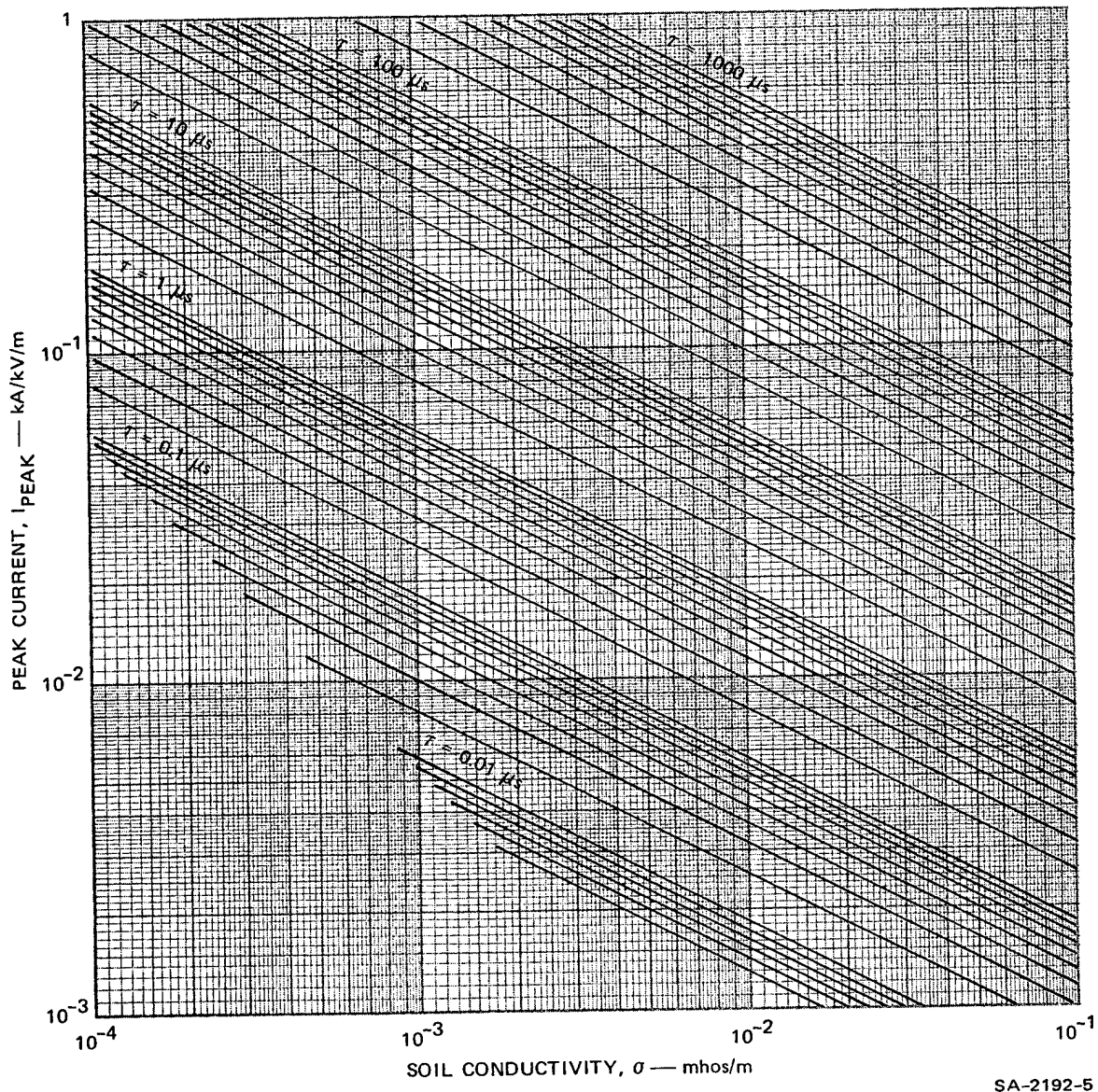
part of the graph where $\tau = \tau_e$. The responses given in this section are valid only if $\tau > \tau_e$. Where the approximations used here are valid, the peak current is inversely proportional to the square root of the soil conductivity (i.e., $\sqrt{\sigma} I_0 = \text{constant}$).

Example: Find the current induced in a buried cable by a horizontally polarized exponential pulse of 10 kV/m with a decay time constant of $1\mu\text{s}$ incident from an elevation angle of



SA-2192-6

FIGURE 4 VARIATION OF PEAK CABLE CURRENT AS AZIMUTH (ϕ) AND ELEVATION (ψ) ANGLES OF INCIDENCE CHANGE [$D(\psi, \phi)$]



SA-2192-5

FIGURE 5 PEAK CABLE CURRENT AS A FUNCTION OF SOIL CONDUCTIVITY AND INCIDENT EXPONENTIAL PULSE-DECAY TIME CONSTANT τ [$D(\psi, \varphi) = 1$]

30 degrees and an azimuth angle of 70 degrees. The soil conductivity is 10^{-3} mho/m.

From Figure 5 we find that for $\sigma = 10^{-3}$ and $\tau = 1 \mu\text{s}$, the peak current is 5.7×10^{-2} kA/kV/m when $D(\psi, \varphi) = 1$. Therefore, for 10 kV/m, the peak current will be 0.57 kA when $D(\psi, \varphi) = 1$. From Figure 4, we find that for horizontal polarization with $\psi = 30^\circ$ and $\varphi = 20^\circ$, $D(\psi, \varphi) = 0.47$. Therefore the peak current for our angle of incidence will be $0.47 \times 0.57 = 0.27$ kA, and the peak will occur $0.85 \tau = 0.85 \mu\text{s}$ after the beginning of the current pulse.

3. Theoretical Basis

The incident electric field $E_o e^{-t/\tau}$ has the Fourier (or Laplace) transform

$$E(\omega) = \frac{E_o}{j\omega + 1/\tau} \quad (18)$$

The resultant z-component of this field at the surface of the ground for horizontal polarization is

$$\begin{aligned} E_z &= (1 + R_h) E(\omega) \sin \varphi \\ &\approx 2 \sqrt{\frac{j\omega \epsilon_o}{\sigma}} E(\omega) \sin \psi \sin \varphi \quad (\sigma \gg \omega \epsilon_o) \end{aligned} \quad (19)$$

and for vertical polarization it is

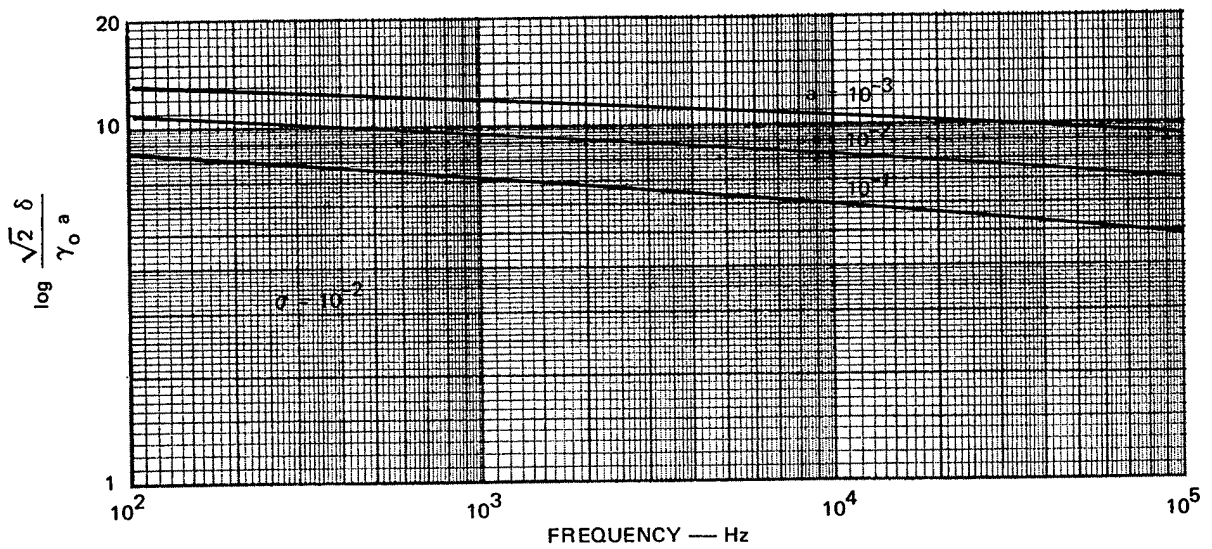
$$\begin{aligned} E_z &= (1 - R_v) E(\omega) \cos \varphi \quad (\sigma \gg \omega \epsilon_o) \\ &\approx 2 \sqrt{\frac{\epsilon_o}{\sigma}} \sqrt{j\omega} E(\omega) \cos \varphi \quad (\sigma \gg \omega \epsilon_o) \end{aligned} \quad (20)$$

where R_h and R_v are the reflection coefficients for oblique incidence on the air/soil interface.

where a is the radius of the cable sheath, $\gamma_0 = 1.781 \dots$, and

$$\gamma = \left[j\omega\mu_0 (\sigma + j\omega\mu) \right]^{\frac{1}{2}} \approx \frac{1 + j}{\delta} \quad \sigma \gg \omega\epsilon \quad (24)$$

To obtain the final expression above, use was made of the fact that $\log(\sqrt{2}\delta/\gamma_0 a) \approx 10$ for a wide range of soil conductivities, conductor radii, and frequencies (see Figure 6).



SA-2192-7

FIGURE 6 VARIATION OF $\log(\sqrt{2}\delta/\gamma_0 a)$ WITH FREQUENCY AND CONDUCTOR RADIUS. (Note that a factor of 10 in conductor radius produces the same effect as a factor of 100 in soil conductivity.)

Using this expression for Z in Eq. (22) and dropping the exponential term, the current becomes

$$\begin{aligned} I(z, \omega) &= \frac{\pi E}{j\omega\mu_0 Z} \\ &= \frac{2\pi\sqrt{\tau}}{5\mu_0\sqrt{j\omega}} \frac{E_0 D(\psi, \varphi)}{j\omega + 1/\tau} \end{aligned} \quad (25)$$

Visualizing the buried cable as a long (or infinite) lossy transmission line, the current far from the ends of the line is

$$I(z, \omega) = P(z)e^{-\gamma z} + Q(z)e^{\gamma z} \quad (21)$$

where

$$P(z) = \frac{E}{2Z_0} \int_0^z e^{\gamma z} e^{-jk'z} dz$$

$$Q(z) = \frac{E}{2Z_0} \int_z^{\ell} e^{-\gamma z} e^{-jk'z} dz$$

For $|\gamma z| \gg 1$ and $\gamma(\ell - z) \gg 1$ (i.e., for points several soil skin depths from either end of the cable), the current is

$$I(z, \omega) \approx \frac{E}{Z} e^{-jk'z} \quad (22)$$

The exponential term gives the phase of the incident field, which is not important in this discussion. The impedance Z is the impedance per unit length of the cable and soil as a transmission line. This impedance is dominated by the impedance of the soil, which is given by

$$\begin{aligned} Z &\approx \frac{-j\gamma}{2\pi a \sigma} \frac{H_0^{(1)}(j\gamma a)}{H_1^{(1)}(j\gamma a)} \\ &\approx \frac{1}{\pi \sigma \delta^2} \left(\frac{\pi}{4} + j \log \frac{\sqrt{2\delta}}{\gamma_0 a} \right) \quad |\gamma a| \ll 1 \\ &\approx \frac{j\omega \mu_0}{\pi} \end{aligned} \quad (23)$$

where $\tau_e = \epsilon_o / \sigma$, and $D(\psi, \varphi)$ is the directivity function given in Section II-B-2 above. The inverse transform of the frequency-dependent function in Eq. (25) is

$$\mathcal{F}^{-1} \left[\frac{1}{\sqrt{j\omega} (j\omega + 1/\tau)} \right] = \sqrt{\tau} e^{-t/\tau} \frac{2}{\sqrt{\pi}} \int_0^{\sqrt{t/\tau}} e^{-u^2} du \quad (26)$$

so that

$$i(z, t) = 10^6 \sqrt{\tau_e} E_o D(\psi, \varphi) e^{-t/\tau} \frac{2}{\sqrt{\pi}} \int_0^{\sqrt{t/\tau}} e^{-u^2} du \quad (27)$$

when $\mu_o = 4\pi \times 10^{-7}$.

Useful insight into the physics of the coupling process can be obtained by using the second expression in Eq. (23) for the impedance of the soil and noting that $\log(\sqrt{2} \delta / \gamma_o a) \gg \pi/4$. Putting this value in Eq. (22) and, again, dropping the exponential phase term, the current in the cable is seen to be

$$I(z, \omega) \approx \frac{\sigma E_z \pi \delta^2}{j \log \frac{\sqrt{2} \delta}{\gamma_o a}} \quad (28)$$

Note that σE_z is the current density in the soil (if the cable were absent) and $\pi \delta^2$ is the area of a circle one skin-depth in radius in the soil. Thus the total current induced in the cable is approximately proportional to the current that would flow in a circular cylinder of soil one skin depth in radius if the cable were not present.

For cables with thin insulation over the shield, the impedance Z per unit length is

$$\begin{aligned}
Z &= Z_{is} + j\omega L \\
&= R_s + j\omega(L_s + L)
\end{aligned}
\tag{29}$$

where, for $\delta/a \gg 1$,

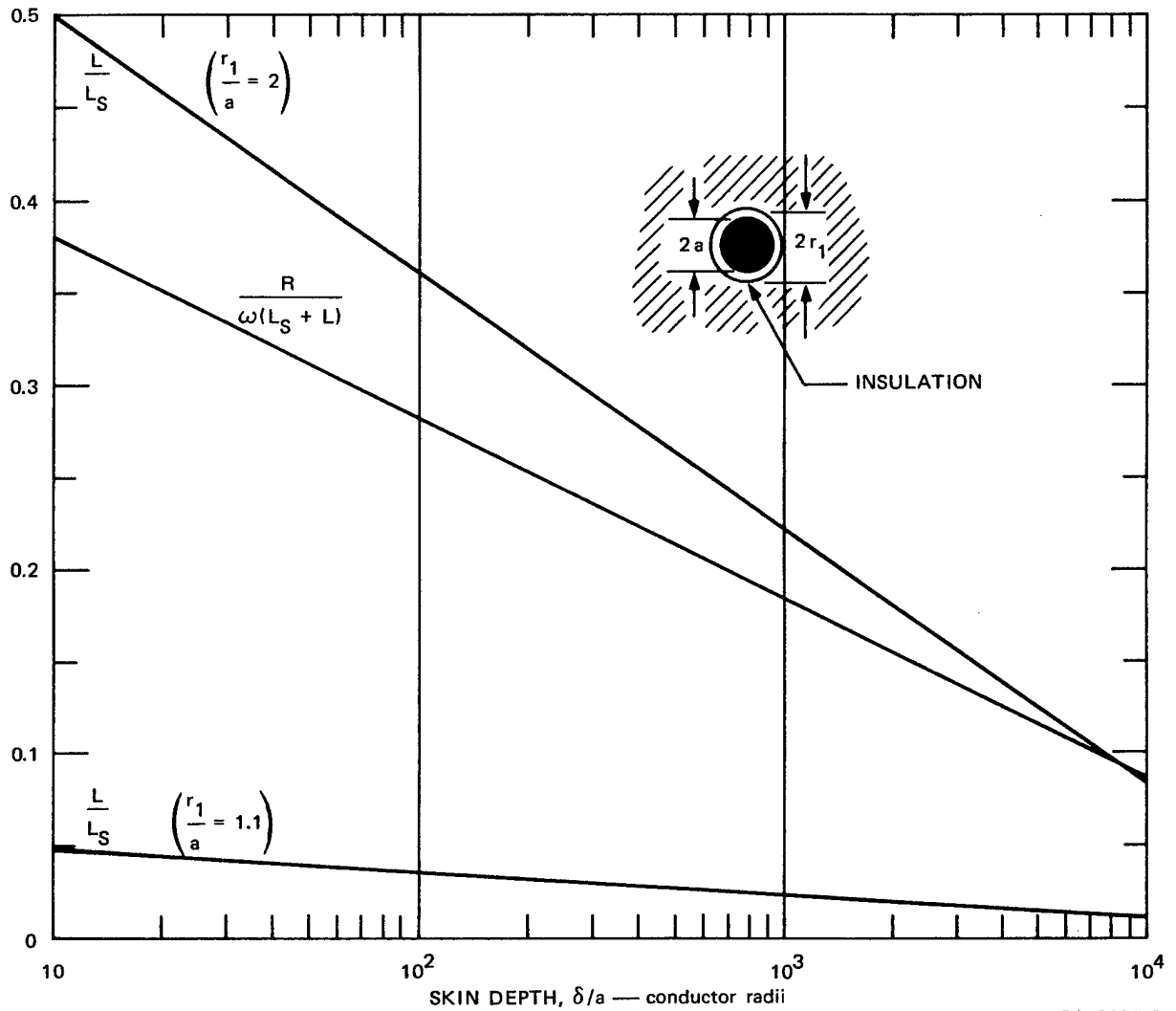
$$R_s = \frac{1}{4\sigma\delta^2} = \frac{\omega\mu}{8} \tag{30}$$

$$L + L_s = \frac{\mu}{2\pi} \log \frac{\sqrt{2}\delta}{\gamma_o a} \tag{31}$$

A plot of $R/\omega(L_s + L)$ and L_s/L in Figure 7 illustrated the relative magnitudes of the resistance and reactance of the impedance per unit length. The ratio of the inductance due to the insulation to that due to the soil outside the insulation in Figure 4 shows that most of inductance is attributable to the soil even at high frequencies (δ/a small), and for a typical insulating jacket thickness of the order of 10 percent of the cable radius, over 90% of the inductance is attributable to the soil. For cables a few centimeters in diameter and soil skin depths of 10 meters or more, the resistance is less than one-fifth the inductive reactance. Therefore, for many practical cases we may use the approximation $R \ll \omega(L + L_s)$ to simplify the solutions to the buried-cable analysis. The propagation factor for the cable/earth transmission line is

$$\gamma = \sqrt{j\omega C [R_s + j\omega(L_s + L)]} \tag{32}$$

Because $C(L_s + L) \gg CL$, the propagation factor is large compared to $k \cos \varphi \cos \psi$, and the results obtained for the bare cable, assuming $|\gamma| \gg k$, are, to a good approximation, also applicable to a cable with a thin insulating jacket.



SA-2192-8

FIGURE 7 VARIATION OF L/L_s AND $R/\omega(L + L_s)$ WITH δ/a FOR AN INSULATED BURIED CABLE. (L is the inductance of the insulation gap, L_s is the inductance of the soil, and R is the soil resistance, all on a per-unit-length basis.)

C. Current Near the End of a Long Bare Cable

1. Class of Problems

The response characteristic presented here are for points near the end of a long (semi-infinite) bare cable. The bulk current in the cable is based on the assumption that the cable sheath is in contact with the soil and that the end of the cable is terminated in a very low

impedance (short circuit) or a very high impedance (open circuit) compared to the characteristic impedance. The short-circuit case might be representative of a cable that is terminated in a large counterpoise or similar low-impedance structure. The open-circuit case is representative of a cable shield that is dead-ended or insulated at the end of the cable. The assumptions that $\sigma > \omega\epsilon$ and $a < \delta$ used for the long bare cable above apply to these cases as well. The results are presented for an exponential pulse with decay time constant τ that is large compared to the soil time constant $\tau_e = \epsilon_0/\sigma$. The electromagnetic pulse is incident from a direction defined by an elevation angle ψ measured from horizontal and an azimuth angle ϕ measured from the axis of the cable (see Figure 1).

2. Response Characteristics

The total current induced near the end of a long cable that is short-circuited is identical to the current far from the ends and is given by Eqs. (14) and (15), and has the waveform shown in Figure 3.

The total current induced near the end of a long cable that is open-circuited at the end by an incident exponential pulse $E_0 e^{-t/\tau}$ is given by

$$I(z, \omega) \approx I_0 \frac{1 - e^{-\sqrt{j\omega/\tau} z/c}}{\sqrt{j\omega\tau} (j\omega + j/\tau)} \quad (33)$$

in the frequency domain, and by

$$i(z, t) \approx I_0 e^{-t/\tau} \frac{2}{\sqrt{\pi}} \int_0^{\sqrt{t/\tau}} \left(1 - e^{-p/u^2}\right) e^{-u^2} du \quad (34)$$

in the time domain, where

$$I_o = 10^6 \sqrt{\tau_e \tau} E_o D(\psi, \varphi) \text{ (amperes)}$$

$$\tau_e = \frac{\epsilon_o}{\sigma} = \text{Time constant of soil (seconds)}$$

τ = Decay time constant of incident pulse (seconds)

E_o = Peak electric-field strength of incident pulse (V/m)

$D(\psi, \varphi)$ = $\cos \varphi$ for horizontal polarization

= $\sin \psi \sin \varphi$ for vertical polarization

z = Distance from end of cable (meters)

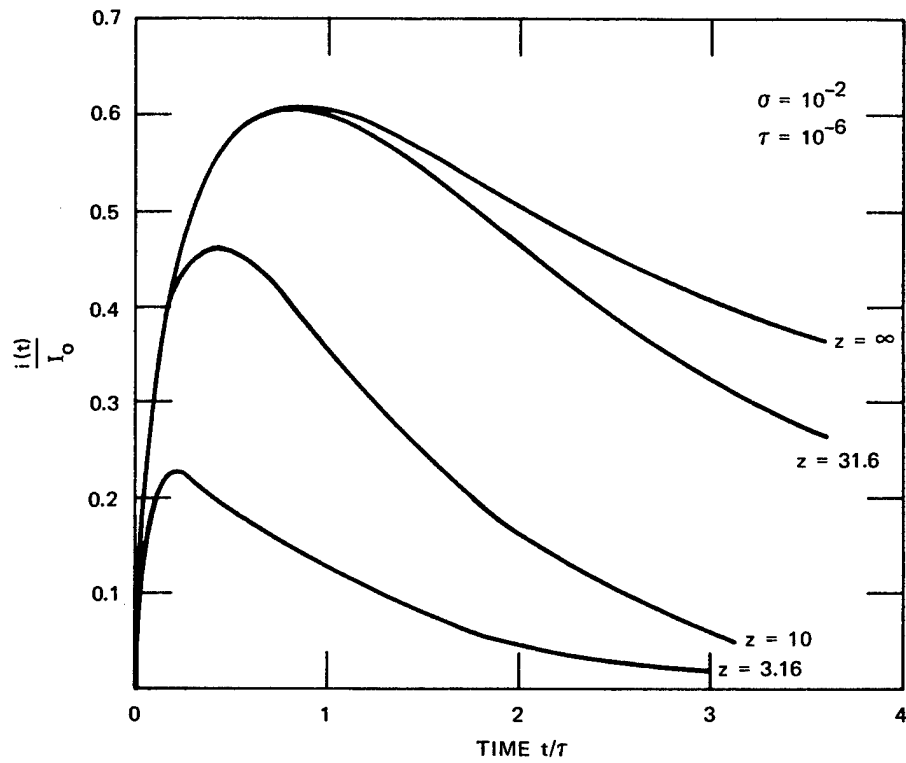
$$c = 1/\sqrt{\mu_o \epsilon_o} = \text{Speed of light in free space}$$

$$p = \left(\frac{z}{c}\right)^2 \frac{1}{4\tau\tau_e} .$$

This current is zero (very small) at the end ($z = 0$) and approaches the value given by Ea. (15) at large distances from the end. Plots of the waveform at distances of 3.16, 10, and 31.6 meters from the end of the cable are shown in Figure 8 for a soil conductivity of 10^{-2} mho/m. Since the waveform is determined by $\frac{1}{\tau_e} (z/c)^2 = \sigma z^2 / \epsilon_o c^2$, the waveforms shown in Figure 8 will represent different distances from the end of the cable if the soil conductivity differs from 10^{-2} mho/m. The magnitude of the current remains inversely proportional to the square root of the soil conductivity ($\sqrt{\sigma} I_o \approx \text{constant}$).

3. Theoretical Basis

The component of the electric field along the cable is given by Eqs. (19) and (20). This field induces a current in the semi-infinite cable extending from $z = 0$ to $z = l \rightarrow \infty$, which is given by Eq. (8), where



SA-2192-9

FIGURE 8 WAVEFORM OF CABLE CURRENT NEAR THE END WHEN SHEATH IS OPEN-CIRCUIT

$$K_1 = -\rho_1 Q(0) \quad K_2 = 0$$

$$P(z)e^{-\gamma z} = \frac{E e^{-jk'z}}{2Z_o \gamma} \frac{1 - e^{-(\gamma - jk')z}}{1 - jk'/\gamma}$$

$$Q(z)e^{\gamma z} = \frac{E e^{-jk'z}}{2Z_o \gamma} \frac{1}{1 + jk'/\gamma}$$

$$Q(0) = \frac{E}{2Z_o \gamma} \frac{1}{1 + jk'/\gamma}$$

$$\begin{aligned}\rho_1 &= 1 \quad \text{when shield is open-circuited} \\ &= -1 \quad \text{when shield is short-circuited} \\ k' &= k \cos \psi \cos \varphi.\end{aligned}$$

The current near the end at $z = 0$ then becomes

$$I(z, \omega) = \frac{E}{Z} \left[e^{-jk'z} - e^{-\gamma z} \right] \quad (35)$$

for the open-circuited cable, and

$$I(z, \omega) = \frac{E}{Z} e^{-jk'z} \quad (36)$$

for the short-circuited cable. The term $\exp(-k'z) = \exp(-jkz \cos \varphi \cos \psi)$ gives the phase of the incident wave at the point z relative to the phase at the end $z = 0$. Since $k' \ll |\gamma|$, the currents become

$$I(z, \omega) \approx \frac{E}{Z} \left(1 - e^{-\gamma z} \right) \quad (\text{open circuit}) \quad (37)$$

$$I(z, \omega) \approx \frac{E}{Z} \quad (\text{short circuit}) \quad (38)$$

when the phase is referred to the phase of the locally incident field. The short-circuit current is thus the same as the current a great distance from the end [see Eq. (25)]. The current near the open-circuited end of the cable is this current reduced by $(1 - e^{-\gamma z})$, where $\gamma \approx \sqrt{j\omega\mu_0\sigma}$.

For the exponential incident pulse given by Eq. (18) and the impedance per unit length given by Eq. (23), the current near an open circuit is given by

$$I(z, \omega) \approx \frac{2\pi\sqrt{\tau_e} E_o D(\psi, \varphi)}{5\mu_o} \frac{1 - e^{-\sqrt{j\omega/\tau_e} z/c}}{\sqrt{j\omega\tau_e} (j\omega + 1/\tau_e)} \quad (39)$$

where $\sqrt{\mu_o \sigma}$ is written as $1/c\sqrt{\tau_e}$. The first term in the frequency-dependent part of Eq. (39) is similar to Eq. (14) and has an inverse transform similar to Eq. (15). The second term can be written as a convolution of the exponential pulse with the impulse response of the function containing $\exp \sqrt{j\omega} / \sqrt{j\omega}$ obtained from

$$\mathcal{F}^{-1} \left[\frac{e^{-\sqrt{j\omega/\tau_e} z/c}}{\sqrt{j\omega\tau_e}} \right] = \frac{\exp \left[- \left(\frac{z}{c} \right)^2 \frac{1}{4\tau_e t} \right]}{\sqrt{\pi\tau_e t}}, \left(\frac{1}{\sqrt{\tau_e}} \frac{z}{c} \geq 0 \right). \quad (40)$$

The current waveform is then given by

$$i(z, t) = I_o e^{-t/\tau_e} \frac{2}{\sqrt{\pi}} \int_0^{\sqrt{t/\tau_e}} \left(1 - e^{-p/u^2} \right) e^{u^2} du \quad (41)$$

where

$$I_o = 10^6 \sqrt{\tau_e} E_o D(\psi, \varphi)$$

$$p = \left(\frac{z}{c} \right)^2 \frac{1}{4\tau_e \tau_e}$$

THIS PAGE INTENTIONALLY BLANK

III CURRENTS AND VOLTAGES INDUCED ON INTERNAL CONDUCTORS

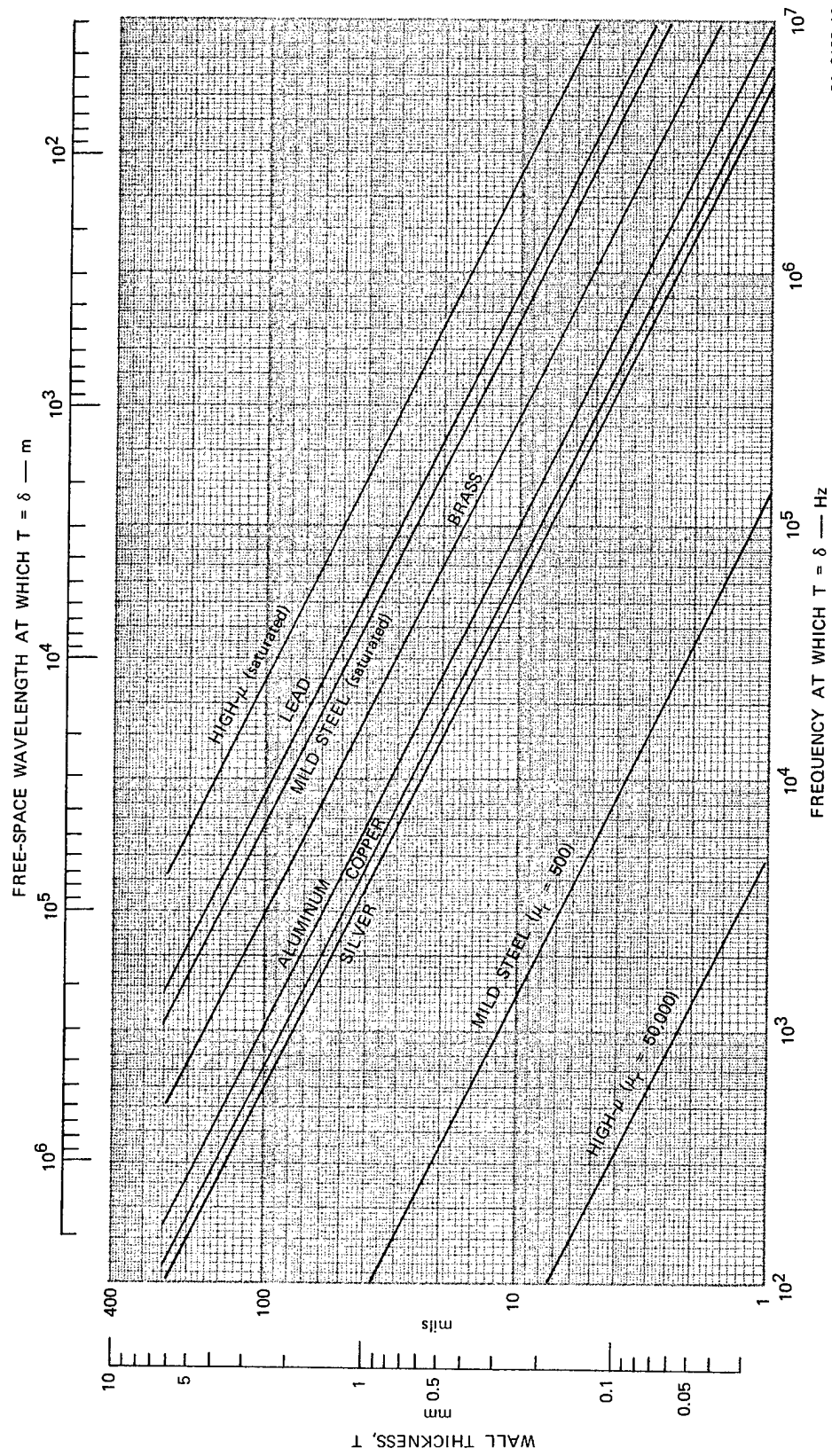
A. General

The internal currents and voltage in this section are presented for exponential currents in the shield of a tubular shielded cable. In Section III-B, the internal currents and voltages are given for cables that are short compared to the shortest wavelength penetrating the shield. In Section III-C, these results are extended to cables that are long compared to the shortest penetrating wavelength, neglecting attenuation of signals propagating on the core. In both sections, the results are presented for shield-current-decay time constants τ that are short, intermediate, and long compared to the shield diffusion time constant τ_s . In Section III-D, some results are presented for the case in which shield currents induced in a buried cable, determined from a wave incident on the surface of the ground, are used to compute the internal currents.

B. Electrically Short Cable with Tubular Shield (Cable Current Given)

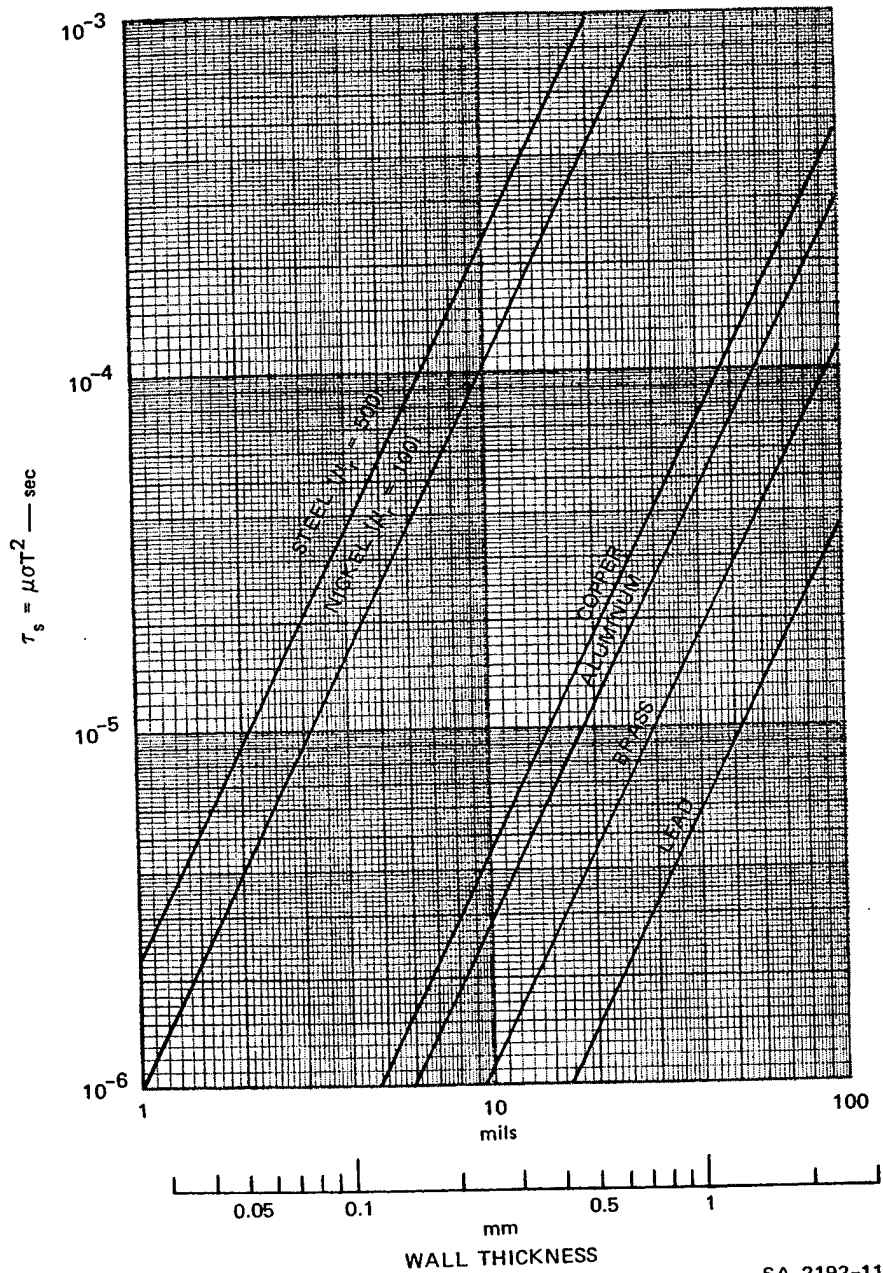
1. Class of Problems

The type of shield considered here is a tubular shield with no holes and no seams that are not continuously welded, brazed, or soldered. The results are not applicable to braided-wire or tape-wound shields. The cables are electrically short at the shortest wavelength penetrating the shield (see Figure 9). The results are given for zero-rise-time exponential pulses; however, these results are applicable to finite-rise-time pulses if the pulse rise time is short compared to the diffusion time (see Figure 10). The open-circuit voltage between the core and the



SA-2192-10

FIGURE 9 FREQUENCY AT WHICH THE SHIELD WALL THICKNESS T IS ONE SKIN DEPTH FOR VARIOUS METALS



SA-2192-11

FIGURE 10 THE DIFFUSION CONSTANT τ_s AS A FUNCTION OF WALL THICKNESS FOR COMMON SHIELDING MATERIALS

shield at the ends of the cable is presented for a given exponential pulse of current flowing in the cable shield. Also presented is the current in the core when the terminating impedance between the core and shield at each end is the common-mode characteristic impedance of the core-to-shield transmission line.

2. Response Characteristics

For a cable of total length ℓ whose shield has a dc resistance per unit length R_o and a current $I_{so} e^{-t/\tau}$ flowing in it, the open-circuit voltage developed between the core and the shield at the end of the cable is

$$V(\omega) = \frac{I_{so} R_o \ell}{2} \frac{\sqrt{j\omega\tau_s}}{\left(j\omega + \frac{1}{\tau}\right) \sinh \sqrt{j\omega\tau_s}} \quad (42)$$

where

$$R_o = (2\pi a \sigma T)^{-1} = \text{dc resistance per meter of the shield}$$

$$\tau_s = \mu \sigma T^2 = \text{Diffusion time constant for the shield (see Figure 10)}$$

$$\tau = \text{Decay time constant of the exponential pulse of shield current.}$$

The quantities a , σ , μ , and T are the radius, conductivity, permeability, and wall thickness of the shield, respectively. The voltage waveform is

$$V(t) = V_o f(t)$$

where

$$f(t) = \mathcal{F}^{-1} \left[\frac{\sqrt{j\omega\tau_s}}{\left(j\omega + \frac{1}{\tau}\right) \sinh \sqrt{j\omega\tau_s}} \right] \text{ and } V_o = \frac{I_{so} R_o \ell}{2} .$$

The function $F(t)$ is plotted in Figure 11 for $\tau = \tau_s$ and for $\tau \gg \tau_s$. For $\tau \ll \tau_s$ the function $f_0(t)$ (τ_s/τ) is plotted. The coefficient V_0 (per kilometer) is plotted in Figure 12 as a function of shield thickness and diameter for copper, aluminum, steel, and lead shield. The peak open-circuit voltages are

$$\begin{aligned} v(t)_{\text{peak}} &= V_0 & (\tau \gg \tau_s) & \quad (43) \\ &= 5.9 \frac{\tau}{\tau_s} V_0 & (\tau \ll \tau_s) \\ &= 0.77 V_0 & (\tau = \tau_s) \end{aligned}$$

if the core is open-circuited (relative to the shield) at both ends. The 10-to-90-percent rise time for the voltage is

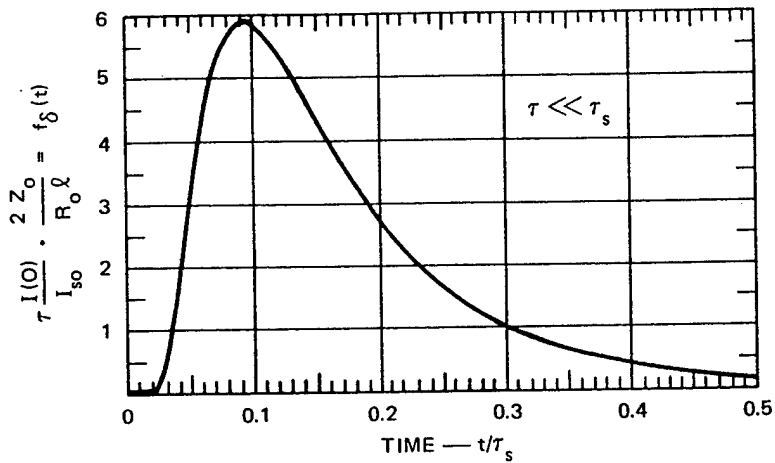
$$\begin{aligned} t_{10-90} &= 0.236 \tau_s & (\tau \gg \tau_s) & \quad (44) \\ &= 0.038 \tau_s & (\tau \ll \tau_s) \\ &= 0.15 \tau_s & (\tau = \tau_s) \end{aligned}$$

Plots of the asymptotic values of the peak voltage and rise time against τ/τ_s are shown in Figure 13 as solid lines, and an estimate of their behavior between asymptotes is shown as a dashed curve.

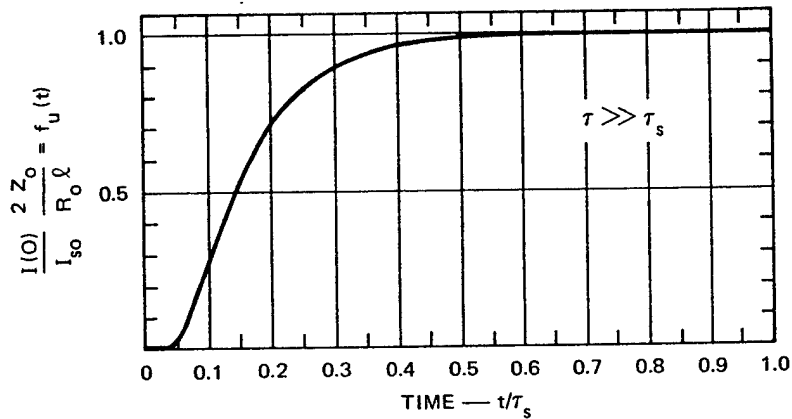
The voltage has the same magnitude and shape at both ends of the cable; however, the polarity at one end is opposite to the polarity at the other end. If the core is shorted to the shield at one end, the open-circuit voltage at the opposite end will have the same waveform but it will double in magnitude.

The current through matched terminations at the ends of the cable will be

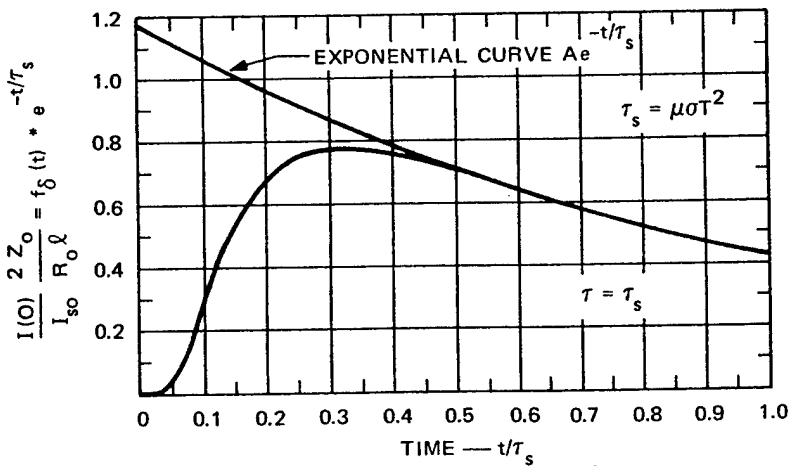
$$I(\omega) = V(\omega)/Z_0 \quad (45)$$



(a) IMPULSE RESPONSE [$\tau I_{so} \delta(t)$]



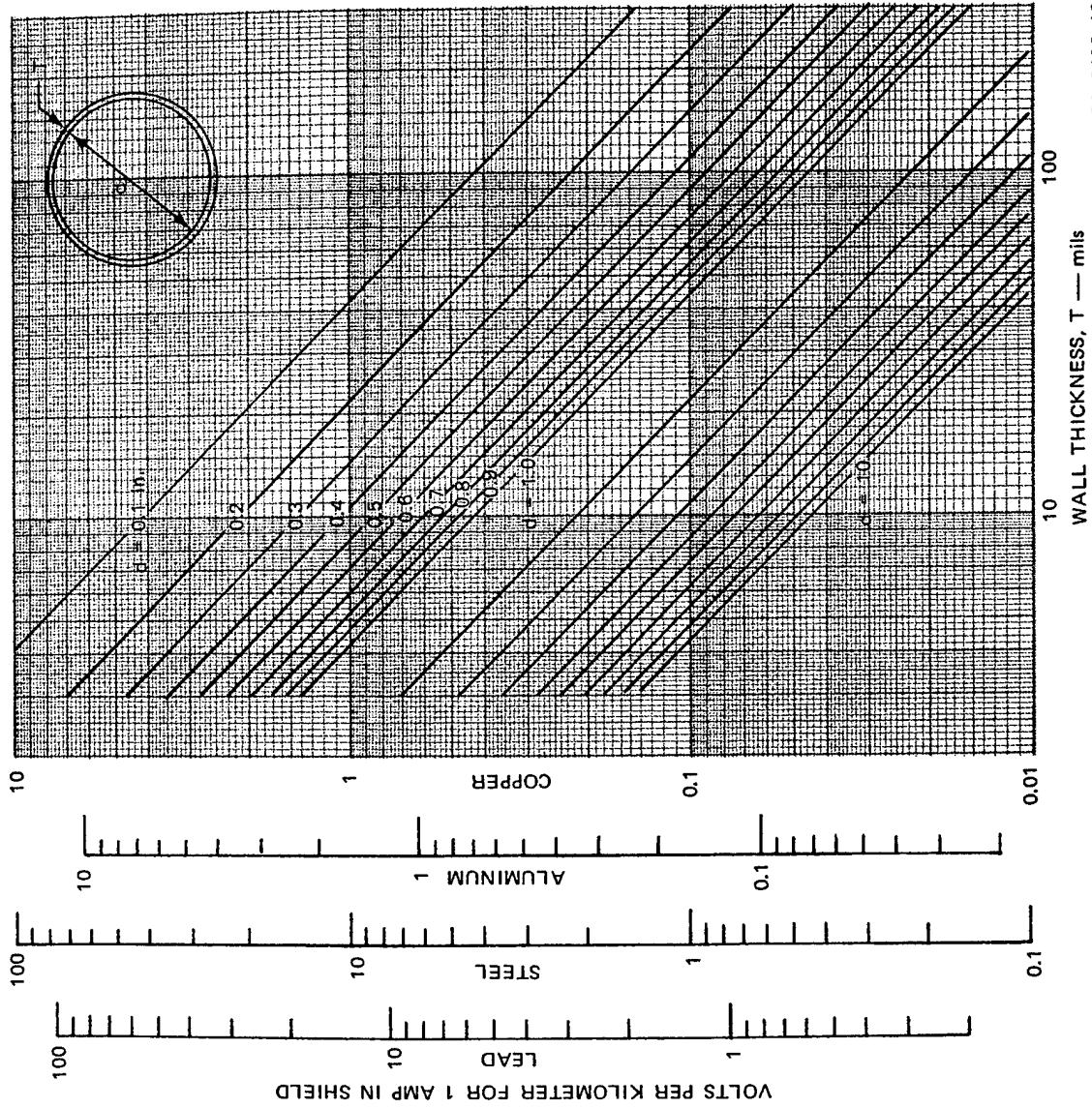
(b) STEP FUNCTION RESPONSE [$I_{so} u(t)$]



(c) EXPONENTIAL RESPONSE [$I_{so} e^{-t/\tau_s}$]

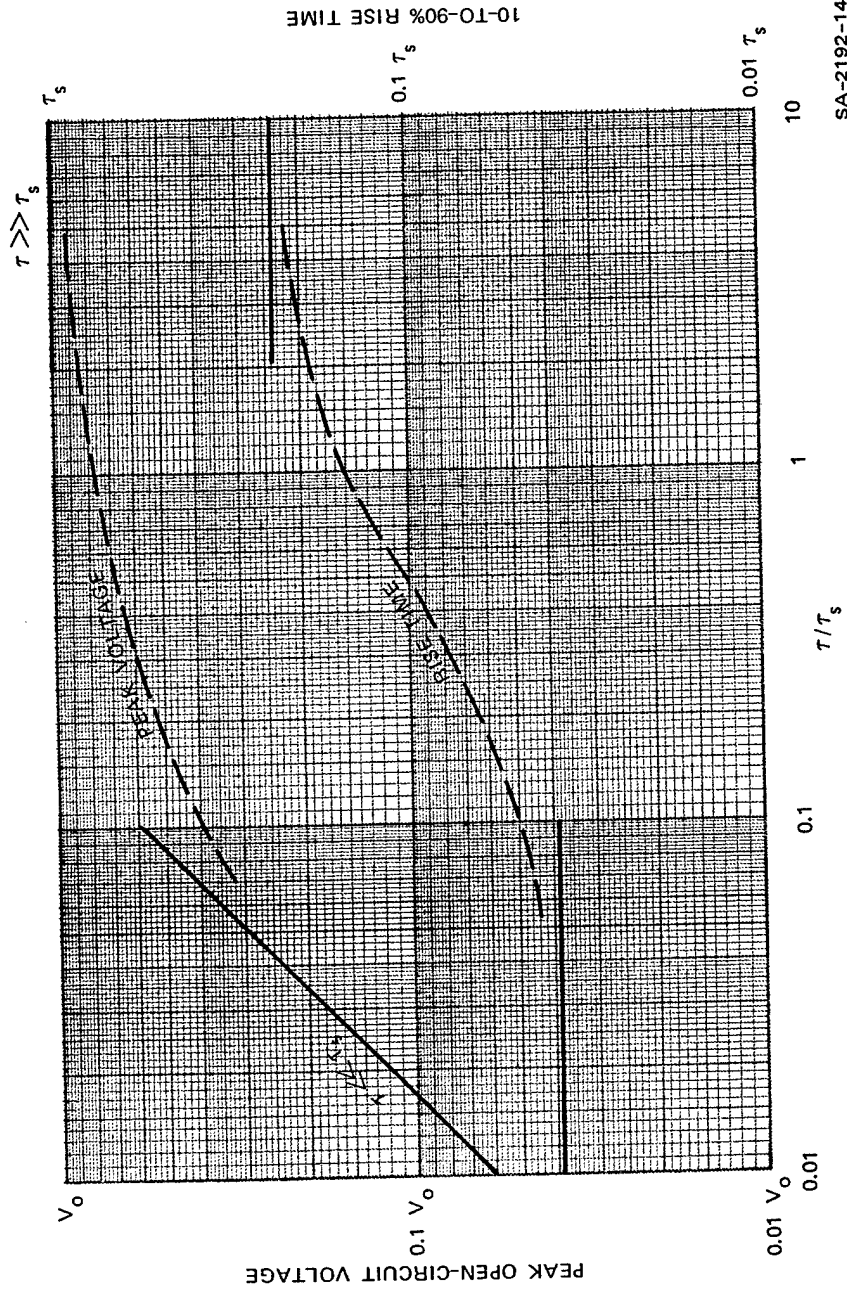
SA-2192-12

FIGURE 11 CORE CURRENT WAVEFORMS PRODUCED BY AN EXPONENTIAL PULSE $I_{so}e^{-t/\tau}$ OF CURRENT IN THE SHIELD (normalized to $V_o/Z_o = I_{so}R_o\ell/2Z_o$)



SA-2192-13

FIGURE 12 OPEN-CIRCUIT VOLTAGE $V_0 = I_{50} R_0 \ell / 2$ BETWEEN CORE AND SHIELD FOR COMMON SHIELDING MATERIALS, THICKNESSES, AND DIAMETERS (for $I_{50} = 1$ ampere and $\ell = 1$ kilometer)



SA-2192-14

FIGURE 13 VARIATION OF PEAK OPEN-CIRCUIT VOLTAGE AND RISE TIME OF CORE-TO-SHIELD VOLTAGE AS A FUNCTION OF EXPONENTIAL SHIELD-CURRENT-DECAY TIME CONSTANT τ (normalized to diffusion constant τ_s)

or

$$i(t) = v(t)/Z_o$$

where Z_o is the common-mode characteristic impedance of the core-to-shield transmission line. This current will be the same magnitude, waveshape, and polarity throughout the length of the cable for the electrically short cables considered here. Thus, all of the data for the open-circuit voltage can be used to obtain core current if the characteristic impedance Z_o can be obtained.

Example: A lead-sheathed cable 2 inches in diameter with a 100-mil-thick sheath is two miles (3.2 km) long and is subjected to an exponential sheath current of 1000 amperes whose decay time constant is 1 μ s. Find the peak open circuit voltage developed at the ends of the cable.

From Figure 9, $T = \delta$ for the lead sheath when $f = 9$ kHz or $\lambda = 33$ km, so the 3.2-km segment is electrically short for the penetrating frequencies. From Figure 10, the diffusion time constant $\tau_s = 3.5 \times 10^{-5}$ seconds, which is much larger than τ , and $\tau/\tau_s = 2.86 \times 10^{-2}$. Therefore, the peak voltage is approximately $(\tau/\tau_s) V_o$. From Figure 12, V_o is 0.55 volts/km for 1 ampere, or $V_o = 0.55 \times 1000 \times 3.2 \approx 1760$ volts, and from Figure 13 the peak voltage is about $0.16 V_o \approx 280$ volts. The 10-to-90-percent rise time from Figure 13 is $0.038 \tau_s = 1.33 \times 10^{-6}$ seconds. The waveform would be that shown in Figure 11(a).

3. Theoretical Basis

The thin-walled tubular shield of radius a , wall thickness T , conductivity σ , and permeability $\mu = \mu_r \mu_o$ has a transfer impedance given

by

$$\begin{aligned}
 Z_T &= \frac{1}{2\pi a \sigma T} \frac{\sqrt{j\omega\mu\sigma} T}{\sinh \sqrt{j\omega\mu\sigma} T} \\
 &= R_o \frac{\sqrt{j\omega\tau_s}}{\sinh \sqrt{j\omega\tau_s}} \quad (46)
 \end{aligned}$$

where $R_o = (2\pi a \sigma T)^{-1}$ is the dc resistance per unit length of the shield and $\tau_s = \mu\sigma T^2$ is a time constant for diffusion through the shield. For cables that are short compared to the shortest wavelength that penetrates the shield, the current induced in internal conductors that are terminated in their characteristic impedance Z_o at both ends of the cable by a current I_s flowing in the shield is

$$I(\omega) = \frac{I_s R_o \ell}{2Z_o} \frac{\sqrt{j\omega\tau_s}}{\sinh \sqrt{j\omega\tau_s}} \quad (47)$$

where ℓ is the length of the cable.

The length ℓ for which this estimate is valid can be ascertained from Figure 10, where the diffusion time constant τ_s is plotted as a function of wall thickness for various shielding metals. When $\tau_s > \ell/c$, the diffusion time is greater than the transit time along the length of the cable, and the entire cable adjusts to the penetrating signal as it is developed. When the diffusion time is less than the transit time, the propagation times to various parts of the cable become significant and transmission-line theory must be used. An alternative method of determining the validity of the short-line approximation, which is applicable to the frequency domain, makes use of Figure 9, which is a plot of the frequency at which the skin depth in the shield is equal to the wall thickness. When $T/\delta > 1$, the attenuation by the shield

is large, whereas, when $T/\delta < 1$, the attenuation is small. Therefore, the wavelength at which $T/\delta = 1$ is the shortest wavelength that freely diffuses through the shield. The free-space wavelength associated with the frequency at which $T/\delta = 1$ is indicated on a scale along the top of Figure 9.

When the shield current is an exponential pulse of the form $I_{so} e^{-t/\tau}$, whose transform is

$$I_{so}(\omega) = \frac{I_{so}}{j\omega + 1/\tau},$$

the current in the internal conductors is

$$I(\omega) = \frac{I_{so} R_o \ell}{2Z_o} \frac{\sqrt{j\omega\tau_s}}{\left(j\omega + \frac{1}{\tau}\right) \sinh \sqrt{j\omega\tau_s}}. \quad (48)$$

Note that if $\tau \gg \tau_s$, the significant spectrum of $I(\omega)$ is determined by $j\omega\tau_s$, and $j\omega + 1/\tau \approx j\omega$ in the denominator. The response of the internal conductors is then the step-function response of the shield. If, on the other hand, $\tau \ll \tau_s$, the significant spectrum of $I(\omega)$ is again determined by $j\omega\tau_s$, but now $j\omega + 1/\tau \approx \frac{1}{\tau}$ in the denominator. The response of the internal conductors is then the impulse response of the shield if the impulse is represented by $\tau I_{so} \delta(t)$, where $\delta(t)$ is the unit impulse.

The response waveform of the internal current for the short pulse ($\tau \ll \tau_s$) is thus

$$i(t) = \frac{I_{so} R_o \ell}{2Z_o} \left(\frac{\tau}{\tau_s}\right) \frac{1}{\sqrt{\pi}} \left(\frac{\tau_s}{\tau}\right)^{3/2} \sum_{n=1}^{\infty} \left[\frac{(2n-1)^2 \tau_s}{2t} - 1 \right] \exp \left[-(2n-1)^2 \frac{\tau_s}{4t} \right] \quad (\tau \ll \tau_s) \quad (49)$$

$$= \frac{\tau}{\tau_s} I_{\ell} f_{\delta}(t)$$

$$\text{where } I_{\ell} = \frac{I_{so} R_{\ell}}{2Z_o}$$

and for the long pulse ($\tau \gg \tau_s$) it is

$$i(t) = \frac{I_{so} R_{\ell}}{2Z_o} \frac{2}{\sqrt{\pi}} \left(\frac{\tau_s}{t}\right)^{\frac{1}{2}} \sum_{n=1}^{\infty} \exp\left[-(2n-1)^2 \frac{\tau_s}{4t}\right] \quad (\tau \gg \tau_s) \quad (50)$$

$$= I_{\ell} f_u(t) \quad .$$

The functions $f_{\delta}(t)$ and $f_u(t)$ are plotted in Figure 11, as well as the response for an exponential pulse for which $\tau = \tau_s$.

The voltage developed between the internal conductors and the shield at the ends of the cable when both ends are open-circuited is $Z_o i(t)$, or

$$v(t) = \frac{I_{so} R_{\ell}}{2} \left(\frac{\tau}{\tau_s}\right) f_{\delta}(t) \quad (\tau \ll \tau_s) \quad (51)$$

$$= \frac{I_{so} R_{\ell}}{2} f_u(t) \quad (\tau \gg \tau_s) \quad (52)$$

C. Correction Factor for Long Cables

1. Class of Problems

The results given below permit the peak core current and time-to-peak to be determined for cables of any length. The results are applicable to tubular shields in which an exponential current pulse propagates in one direction only (no reflections). The core-to-shield transmission line is assumed to be lossless (no attenuation) and terminated in its characteristic impedance at its ends.

2. Response Characteristics

The peak current through matched terminations at the end of a shielded cable of any length ℓ , when a current $I_{so} e^{-t/\tau_1}$ flows in the shield, is, for $\tau \ll \tau_s$,

$$i_{\text{peak}} = \frac{I_{so} R_o \ell}{2Z_o} \frac{\tau}{\tau_s} F_\ell \quad (\tau \ll \tau_s) \quad (53)$$

where

$$F_\ell = 5.9 \left(\frac{t_o}{\tau_s} \ll 0.1 \right) \quad (54)$$

$$= \frac{\tau_s}{t_o} \left(\frac{t_o}{\tau_s} > 0.5 \right)$$

$$t_o = \frac{\ell}{c} (\sqrt{\epsilon_r} \pm k'/k)$$

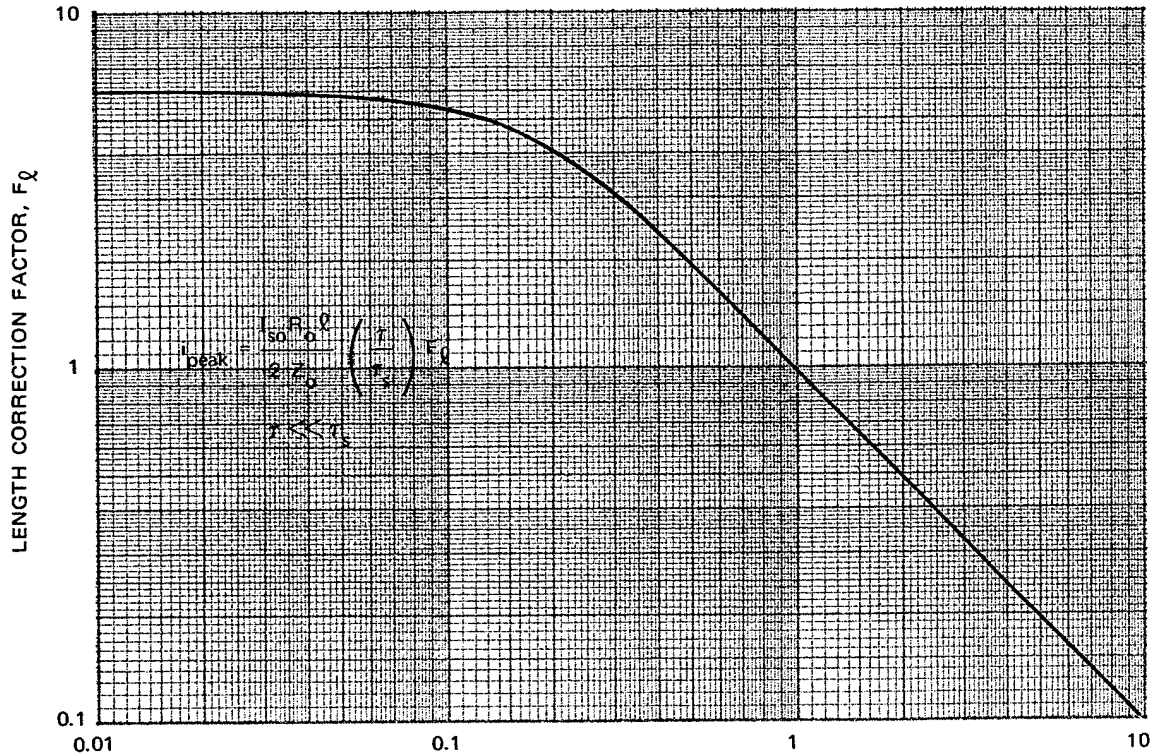
ϵ_r = Dielectric constant of core-to-shield insulation

τ_s = Shield diffusion time constant (see Figure 10)

$k'/k = 1$, if shield current is propagating with velocity c

$= \cos \phi \cos \psi$, if shield current is induced in a buried cable by a wave incident from (ψ, ϕ) (see Figure 1).

The positive sign is used when the direction of propagation of the shield current is away from the terminals, and the negative sign is used when the direction of propagation is toward the terminals at which i_{peak} is to be determined. A plot of F_ℓ as a function of t_o/τ_s is shown in Figure 14.



$$\frac{t_o}{\tau_s} = \frac{l}{C \tau_s} \left(\sqrt{\epsilon_r} \pm \frac{k'}{k} \right)$$

SA-2192-15

FIGURE 14 CORRECTION FACTOR FOR THE PEAK VOLTAGE AND CURRENT INDUCED IN LONG SHIELDED CABLES (k' is the propagation factor for the shield current, $k = \omega \sqrt{\mu_0 \epsilon_0}$, and ϵ_r is the dielectric constant of the core-to-shield insulation)

The time to reach the peak currents is

$$t_{\text{peak}} \approx 0.09 \tau_s \quad \left(\frac{t_o}{\tau_s} \ll 0.1 \right) \quad (55)$$

$$\approx 1.05 t_o \quad \left(0.1 \leq \frac{t_o}{\tau_s} \leq 0.5 \right)$$

$$\approx 0.5 \tau_s \quad \left(\frac{t_o}{\tau_s} > 0.5 \right)$$

The waveform of the current is approximately that of Figure 11(a) for $t_o/\tau_s < 0.1$, and like the leading edge of Figure 11(b) for $t_o/\tau_s > 0.5$. Typical waveforms are shown in Figure 15(a).

The peak voltage across the matched terminations is $i_{\text{peak}} Z_o$ if both ends of the cable are terminated in the characteristic impedance Z_o . The peak open-circuit voltage at one end when the other end is terminated in its characteristic impedance is $2 i_{\text{peak}} Z_o$.

When $\tau \gg t_o$, the peak current in the core is

$$i_{\text{peak}} \approx \frac{I_{so} R_o \ell}{2Z_o} \quad (\tau \gg t_o) \quad (56)$$

and the time to reach the peak (shoulder of the current step) is

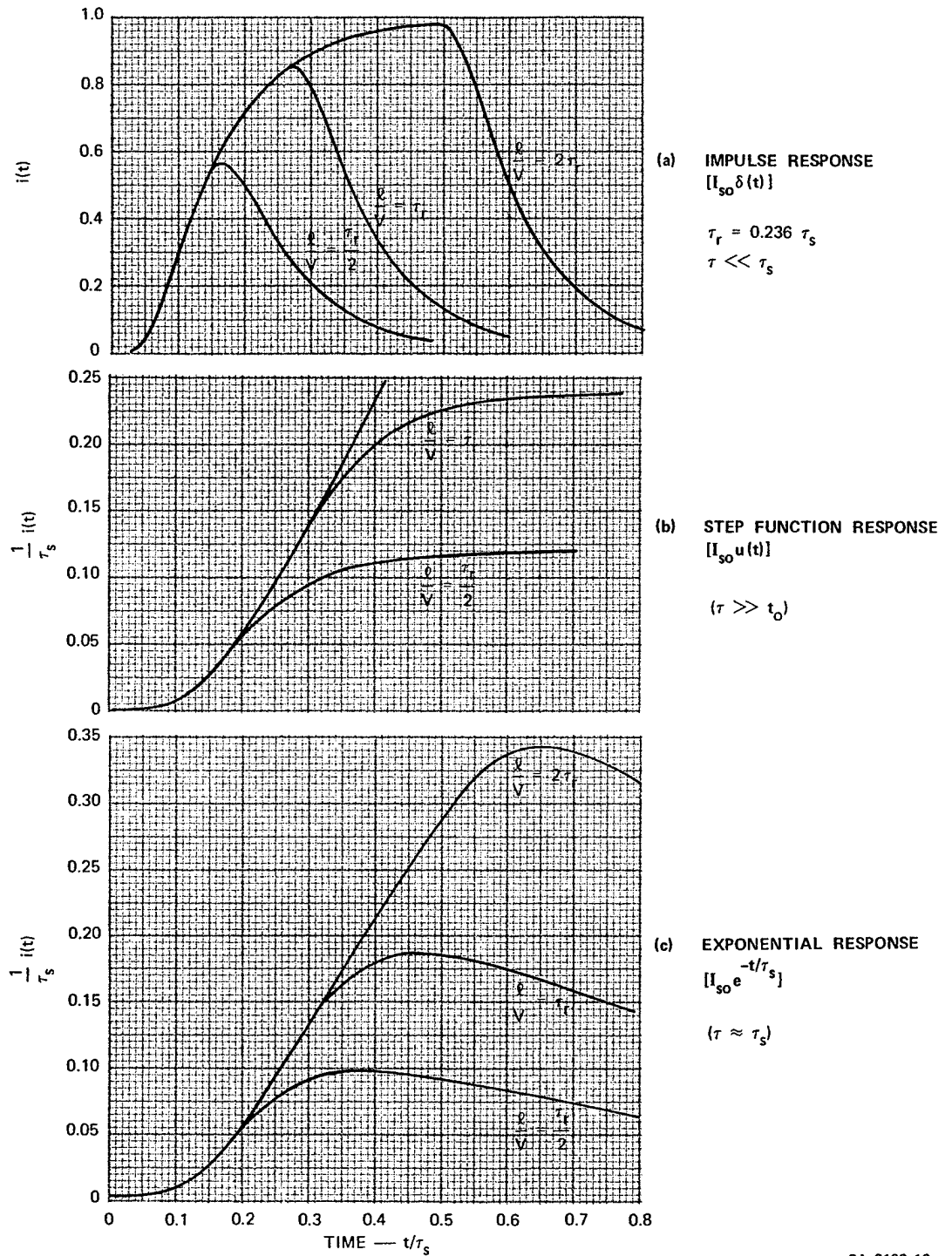
$$t_{\text{peak}} \approx 0.5 \tau_s \quad (t_o \ll \tau_s) \quad (57)$$

$$\approx t_o \quad (t_o \ll \tau_s)$$

Waveforms for the core current are shown in Figure 15 for $\tau \ll \tau_s$, $\tau \gg t_o$, and $\tau = \tau_s$, in terms of $t_o = \ell/v$. The transit time ℓ/v is expressed in terms of the 10-to-90-percent rise time τ_r of the step-function response of a short cable. The value of the 10-to-90-percent rise time is $\tau_r = 0.236 \tau_s$. A plot of t_o for polyethylene insulated cable ($\epsilon_r = 2.3$) and various values of $k'/k = \cos \phi \cos \psi$ is shown in Figure 16. Note that $k'/k = 1$ gives the condition for the shield current propagating with velocity c , regardless of whether the current is induced by an incident wave or by some other means.

3. Theoretical Basis

A cable with a tubular shield is assumed to extend from $z = 0$ to $z = \ell$, and its core is terminated in its characteristic impedance



SA-2192-16

FIGURE 15 CORE-CURRENT WAVEFORMS FOR ELECTRICALLY LONG CABLES WITH AN EXPONENTIAL SHIELD CURRENT $I_{so}e^{-t/\tau}$. (τ_s is the shield diffusion constant, $\tau_r = 0.236 \tau_s$, and $l/v = l\sqrt{\epsilon_r}/c$ is the one-way transit time along the core.)

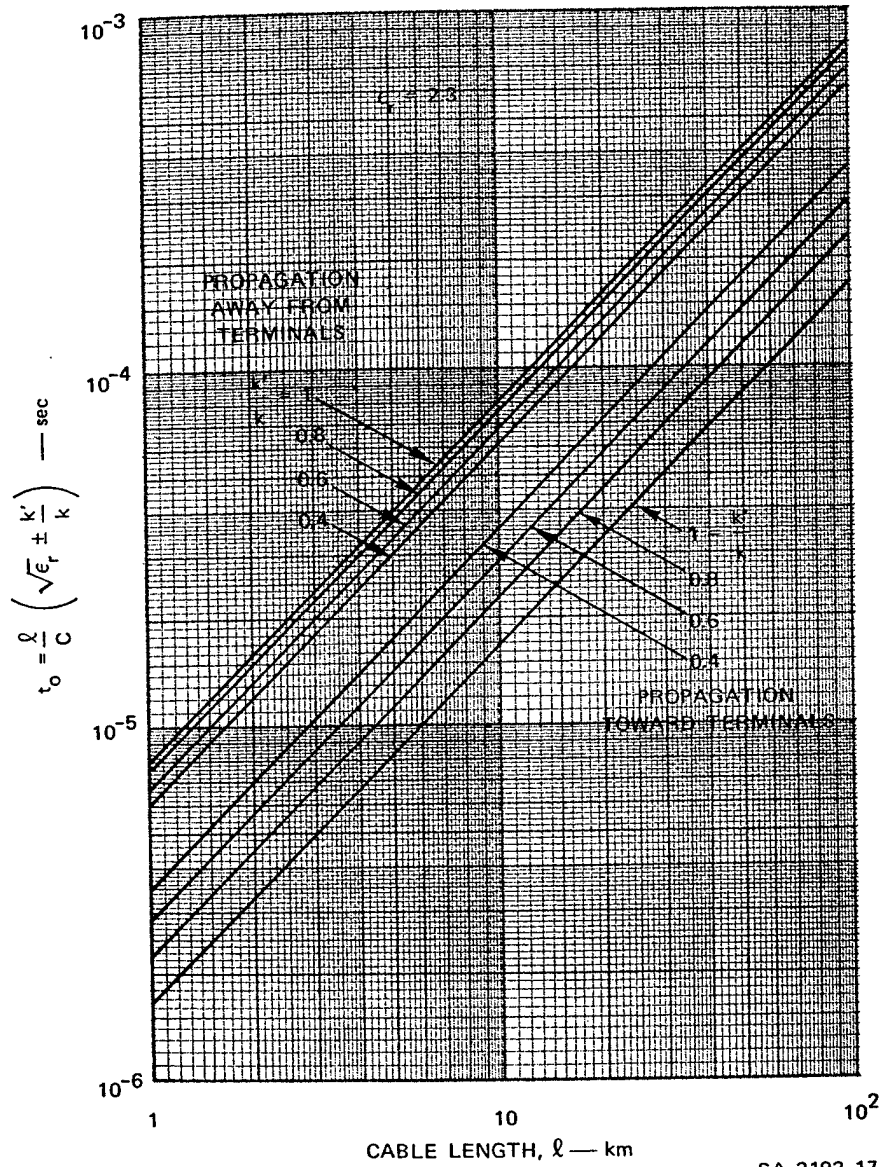


FIGURE 16 DIFFERENTIAL TRANSIT TIME t_0 AS A FUNCTION OF CABLE LENGTH AND PROPAGATION FACTOR k' FOR THE SHIELD CURRENT FOR POLYETHYLENE-INSULATED CABLE CORE

12-16

TH AN
stant,
s.)

at both ends. The shield current is

$$\frac{I_{so} e^{\pm jk'z}}{j\omega + 1/\tau} \approx \tau I_{so} e^{\pm jk'z} \quad (\tau \ll \tau_s) \quad (58)$$

and the core current through the termination at $z = 0$ is, from Eqs. (8) through (13),

$$I(0, \omega) = Q(0)$$

$$\approx \frac{I_{so} R_o}{2Z_o} \frac{\tau \sqrt{j\omega\tau_s}}{\sinh \sqrt{j\omega\tau_s}} \frac{1 - e^{-j\omega t_o}}{j\omega t_o / \ell} \quad (59)$$

where $t_o = \frac{\ell}{c} \left(\sqrt{\epsilon_r} \pm \frac{k'}{k} \right)$, ϵ_r is the dielectric constant of the insulation between the core and the shield, and $k = \omega/c$. The current waveform is thus

$$\begin{aligned} i(0, t) &= \frac{I_{so} R_o \ell}{2Z_o} \frac{\tau}{t_o} [f_u(t) - f_u(t-t_o) u(t-t_o)] \\ &= \frac{I_{so} R_o \ell}{2Z_o} \frac{\tau}{\tau_s} F(t) \end{aligned} \quad (60)$$

where

$$F(t) = \frac{\tau_s}{t_o} [f_u(t) - f_u(t-t_o) u(t-t_o)] \quad (61)$$

The function $f_u(t)$ is plotted in Figure 11(b). From Figure 11(b) it is apparent that for $0.05 \leq t/\tau_s \leq 0.5$, the maximum value of $F(t)$ will occur when $t/\tau_s \approx 1.05 t_o/\tau_s$, and the value of this maximum will be $f_u(1.05 t_o)/(t_o/\tau_s)$. When $t_o \ll \tau_s$, the value of $F(t)$ can be obtained

from the short-cable form of Eq. (59), for which

$$(8) \quad \frac{1 - e^{-j\omega t_o}}{j\omega t_o / \ell} \approx \ell \quad (62)$$

and

$$(8) \quad i(0,t) = \frac{I_{SO} R_o \ell}{2Z_o} \frac{\tau}{\tau_s} f_{\delta}(t) \quad (63)$$

59) The function $f_{\delta}(t)$ is plotted in Figure 11(a) and has a maximum value of 5.9 at $t = 0.09 \tau_s$. Therefore, the value of $F(t)$ that produces the peak value of $i(0,t)$ is

ation
is

$$F_{\ell} \approx 5.9 \quad \left(\frac{t_o}{\tau_s} < 0.1 \right) \quad (64)$$

(60)

$$\approx \frac{f_u(1.05t_o)}{\frac{t_o}{\tau_s}} \quad \left(\frac{t_o}{\tau_s} > 0.05 \right)$$

(61)

$$\approx \frac{1}{\left(\frac{t_o}{\tau_s} \right)} \quad \left(\frac{t_o}{\tau_s} > 0.5 \right) .$$

t is

If the shield current is propagating with the speed of light,
 $k' = k$ and

ned

$$t_o = \frac{\ell}{c} (\sqrt{\epsilon_r} \pm 1) \quad (65)$$

A more interesting case for buried cables, however, is the case in which the shield current is generated by the local incident field. In this case, $k' = k \cos \psi \cos \omega$, and

$$t_o = \frac{\ell}{c} (\sqrt{\epsilon_r} \pm \cos \psi \cos \varphi) .$$

When the pulse time constant τ is large compared to the differential transit time t_o , the response to a step function, which is the integral of the impulse response, is obtained. Thus

$$i(0,t) = \frac{I R \ell}{2Z_o} \int_0^t F(t) dt \quad (\tau \gg t_o) \quad (66)$$

and the step-function of shield current produces a step function of internal current. The rise time of the internal current is not zero, however, as can be seen in Figure 15(b). If t_o is small, the approximation of Eq. (62) leads to

$$i(0,t) \approx \frac{I R \ell}{2Z_o} f_u(t) \quad (t_o \ll \tau_s) \quad (67)$$

while if t_o is not small compared to τ_s , the integration of Eq. (62) leads to

$$i(0,t) \approx \frac{I R \ell}{2Z_o} \frac{t}{t_o} \quad (t \leq t_o) \quad (68)$$

$$= \frac{I R \ell}{2Z_o} \quad (t \geq t_o) .$$

Thus, in either case the peak current is $I R \ell / 2Z_o$, but the time to reach the peak is approximately $0.5 \tau_s$ when $t_o \ll \tau_s$, and is approximately

t_o when t_o is not small compared to τ_s .

D. Internal Voltage from Incident Field

1. Class of Problems

The results presented below give the voltage between the core and the shield induced in a buried cable by an exponential plane-wave pulse incident on the surface of the ground. The results apply to cables that are short compared to the shortest wavelength penetrating the shield (see Figure 9). The cables are assumed to have at least one tubular shield (see Section III-E). The results are obtained from the convolution of the cable current obtained in Section III-B with the impulse response of the tubular shield obtained in Section III-B.

2. Response Characteristics

The open-circuit voltage induced between the core and the shield of a buried, tubular-shielded cable by an incident exponential pulse $E_o e^{-t/\tau}$ is given by

$$V(\omega) = V_o I_o \sqrt{\frac{\tau_s}{\tau}} \frac{1}{(j\omega + 1/\tau) \sinh \sqrt{j\omega\tau}_s} \quad (69)$$

where

$$V_o = \frac{R \ell}{2} \quad [\text{see Eq. (42)}]$$

$$I_o = 10^6 \sqrt{\tau \tau_e} E_o D(\psi, \varphi) \quad [\text{see Eq. (15)}]$$

$\tau_s = \mu\sigma T^2$ is the diffusion constant for the tubular shield.

The open-circuit voltage waveform is

$$v(t) = \frac{V_o I_o}{\sqrt{\pi}} \sqrt{\frac{\tau_s}{\tau}} e^{-t/\tau} \int_0^{t/\tau_s} \left\{ e^{(\tau_s/\tau)y} \sum_{n=1}^{\infty} \frac{n}{y^{3/2}} \exp \left[- \left(\frac{2n-1}{2} \right)^2 \frac{1}{y} \right] \right\} dy \quad (70)$$

This waveform, normalized to $V_o I_o / \sqrt{\pi}$, is plotted in Figure 17 for several values of τ_s / τ .

3. Theoretical Basis

The current induced in a buried cable by an incident exponential field $E_o e^{-t/\tau}$ is given by Eq. (14) as

$$I(\omega) = I_o \frac{1}{\sqrt{j\omega\tau} (j\omega\tau + 1/\tau)} \quad (71)$$

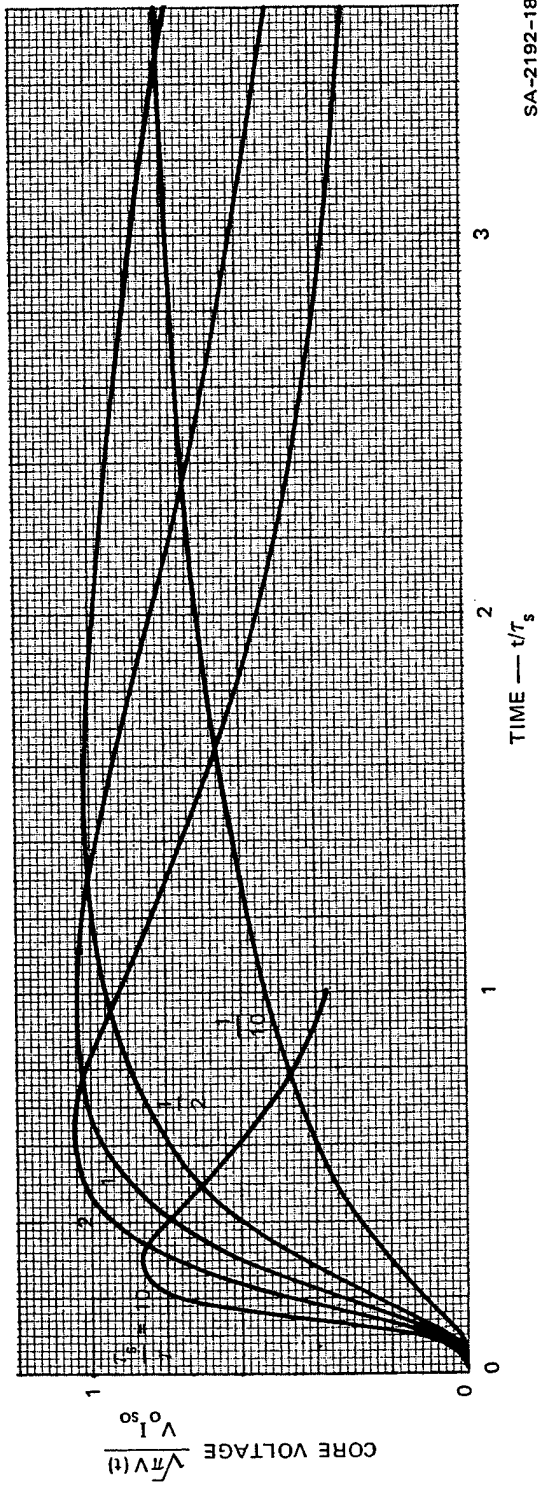
and the open-circuit voltage developed between the core and the shield is given by Eq. (47) as

$$V(\omega) = V_o \frac{\sqrt{j\omega\tau_s}}{\sinh \sqrt{j\omega\tau_s}} \quad (72)$$

for an impulse of shield current. The open-circuit voltage induced by a shield current $I(\omega)$ is therefore

$$V(\omega) = V_o I_o \sqrt{\frac{\tau_s}{\tau}} \frac{1}{(j\omega + 1/\tau) \sinh \sqrt{j\omega\tau_s}} \quad (73)$$

and the open-circuit voltage waveform is



SA-2192-18

FIGURE 17 CORE-TO-SHIELD VOLTAGE WAVEFORMS INDUCED IN BURIED CABLE BY AN INCIDENT PLANE-WAVE EXPONENTIAL PULSE $e^{-t/r}$

$$v(t) = V_o I_o \frac{\tau_s}{\pi\tau} e^{-t/\tau} \int_0^{t/\tau} e^{(\tau_s/\tau)y} \sum_{n=1}^{\infty} \frac{n}{y^{3/2}} \exp \left[- \left(\frac{2n-1}{2} \right)^2 1/y \right] dy. \quad (74)$$

The function $v(t)$ normalized to $V_o I_o / \sqrt{\pi}$ is plotted in Figure 17 for several values of τ_s/τ . The current $i(t)$ through matched terminations on the core is $v(t)/Z_o$.

E. Multiple Shields

1. Class of Problem

The results presented below apply to multiple-shield cables having at least one tubular shield. The remaining shields may be braided wire, tape-wound, or any other leaky shield whose transfer impedance is relatively independent of frequency in the range of frequencies passed by the tubular shield. The results below provide rough approximations for equivalent tubular shields having the same shielding properties as the multiple shield. These equivalent shield characteristics can then be used with the results of Sections III-B, -C, or -D to obtain internal responses.

2. Equivalent Shield Characteristics

A multiple-shield system containing one tubular shield whose transfer impedance is $R_{01} \sqrt{j\omega\tau_s} / \sinh \sqrt{j\omega\tau_s}$ and other shields whose combined resistance per unit length is R_{02} for frequencies between 0 and $1/2\pi \tau_s$ has an equivalent transfer impedance given by

$$Z_T \approx R_{01} \frac{\sqrt{j\omega\tau_s}}{\sinh \sqrt{j\omega\tau_s}} \quad (R_{01} \ll R_{02}) \quad (75)$$

and

$$Z_T \approx R_{02} \frac{\sqrt{j\omega T_s}}{\sinh \sqrt{j\omega T_s}} \quad (R_{01} \gg R_{02}) \quad (76)$$

3. Theoretical Basis

If a cable shield consists of several layers of shielding material, at least one of which is a tubular shield with no holes or seams, the transfer impedance of the composite shield can be written

$$Z_T = \frac{R_{01} R_{02} \frac{\gamma T}{\sinh \gamma T}}{R_{01} \coth \gamma T + R_{02} + j\omega L} \quad (77)$$

where R_{01} is the dc resistance per unit length of the tubular shield of thickness T ; R_{02} is the dc resistance per unit length of the other shields; $\gamma T = \sqrt{j\omega T_s}$; and L is the inductance per unit length between the tubular shield and the other shields. It is assumed that the transfer and internal impedances are relatively independent of frequency when $\gamma T \leq 1$, and it is assumed that ωL is relatively insignificant compared to R_{01} or R_{02} when $\gamma T \leq 1$. Then

$$Z_T \approx \frac{R_{01} R_{02} \gamma T}{R_{01} \cosh \gamma T + R_{02} \sinh \gamma T} \quad (\omega L \ll R_{01}, R_{02}) \quad (78)$$

Now, when $R_{01} \gg R_{02}$,

$$Z_T \approx R_{02} \frac{\gamma T}{\cosh \gamma T} \quad (79)$$

and since $\cosh \gamma T$ and $\sinh \gamma T$ behave the same for large γT , the high-frequency behavior of the transfer impedance is very similar to that of a tubular shield whose dc resistance is R_{02} and whose diffusion

characteristics are those of the tubular shield. The current through matched terminations between the core and shield is, by analogy with Eq. (48),

$$I(\omega) \approx \frac{I_{so} R_{02} \ell}{2Z_o} \frac{\sqrt{j\omega\tau_s}}{(j\omega + \frac{1}{\tau}) \cosh \sqrt{j\omega\tau_s}} \quad (R_{01} \gg R_{02}) \quad (80)$$

where τ_s is determined from the tubular shield parameters, and R_{02} is determined from the other shields. The current waveforms are given by

$$i(t) \approx I_l \frac{\tau}{\tau_s} \frac{1}{\sqrt{\pi}} \frac{\tau}{\tau_s} \sum_{n=1}^{\infty} \frac{(2n-1)^2 \tau_s}{2t} (-1)^{n-1} \exp \left[-\frac{(2n-1)^2 \tau_s}{4t} \right] \quad (\tau \ll \tau_s)$$

$$\approx I_l \frac{2}{\sqrt{\pi}} \frac{\tau_s}{t} \sum_{n=1}^{\infty} (-1)^{n-1} \exp \left[-\frac{(2n-1)^2 \tau_s}{4t} \right] \quad (\tau \gg \tau_s) \quad (81)$$

where $I_l = \frac{I_{so} R_{02} \ell}{2Z_o}$. Comparing these expressions with Eqs. (49) and (50), it is observed that the series above alternates because of the $(-1)^{n-1}$ coefficient, whereas those in Eqs. (49) and (50) do not alternate. Furthermore, it has been found that the first term of the series defines the waveform quite well for times beyond the peak of Figure 11(a) and beyond the shoulder of Figure 11(b). Therefore the alternating terms can affect only the late-time behavior of the waveforms, and then only be reducing the late-time magnitude. Therefore, the waveforms of Figure 11 will be very good approximations to the waveforms induced through the composite shield with $R_{01} \gg R_{02}$.

If $R_{02} \gg R_{01}$, Eq. (77) approaches

$$Z_T \approx \frac{R_{01} \gamma T}{\sinh \gamma T} \quad (R_{02} \gg R_{01}) \quad (82)$$

which is the transfer impedance of the tubular shield alone. In this case, the other shields are not very effective, and the composite shield behaves as though it were a single tubular shield. The results of Section III-B then apply directly to this area.

The quality of the predictions based on these approximations depends on how well the assumptions are met. Generally, the assumptions are of such a nature that the predicted core voltages or currents will be larger, rather than smaller, than the actual voltages and currents induced on the cable core, since all of the predictions involve reducing the size of the denominator in Eq. (77), which increases the transfer impedance.

THIS PAGE INTENTIONALLY BLANK

Appendix A

LIST OF SYMBOLS

THIS PAGE INTENTIONALLY BLANK

Appendix A

LIST OF SYMBOLS

a	Radius of cable shield (meters)
c	Speed of light (3×10^8 meters/second)
C	Capacitance (farads, farads/meter)
$D(\psi, \phi)$	Directivity factor (dimensionless)
e	2.718...
E	Electric-field strength (volts/meter)
f	Frequency (hertz)
G	Conductance (mhos/meter)
i	Instantaneous current (amperes)
I	Monochromatic current (ampere-seconds)
j	Imaginary unit $\sqrt{-1}$
k	Free-space phase factor $\omega\sqrt{\mu_0 \epsilon_0}$ (meter ⁻¹)
K	Constant
l	Cable length (meters)
L	Inductance (henries, henries/meter)
$\left. \begin{matrix} P(z) \\ Q(z) \end{matrix} \right\}$	Source functions (amperes)
r	Radial distance (meters)
R	Resistance (ohms, ohms/meter)
R_v, R_h	Reflection factor for oblique wave incidence (dimensionless)
s	Complex frequency (second ⁻¹)
t	Time (seconds)
T	Shield thickness (meters)
v	Instantaneous voltage (volts)
V	Monochromatic voltage (volt-seconds)

Y	Admittance per unit length (mhos/meter)
z	Distance along axis of cable (meters)
Z	Impedance per unit length (ohms/meter)
Z_0	Characteristic impedance $\sqrt{Z/Y}$ (ohms)
α	Attenuation constant (nepers/meter)
β	Phase factor $k\sqrt{\epsilon_r}$ (meters ⁻¹)
γ	Complex propagation factor (meters ⁻¹)
γ_0	1.781... (Euler's constant)
δ	Skin depth $(\pi f \mu \sigma)^{-\frac{1}{2}}$ (meters)
ϵ	Permittivity $\epsilon_r \epsilon_0$ (farads/meter)
ϵ_0	Permittivity of free space 8.85×10^{-12} (farads/meter)
ϵ_r	Relative permittivity (dimensionless)
η	Intrinsic impedance $\sqrt{\frac{\mu}{\epsilon}}$ (ohms)
λ	Wavelength (meters)
μ	Permeability $\mu_r \mu_0$ (henries/meter)
μ_0	Permeability of free space $4\pi \times 10^{-7}$ (henries/meter)
μ_r	Relative permeability (dimensionless)
ρ	Reflection coefficient (dimensionless)
σ	Conductivity (mhos/meter)
τ	Time constant (seconds)
φ	Azimuth angle of incidence (dimensionless)
ψ	Elevation angle of incidence (dimensionless)
ω	Radian frequency $2\pi f$ (second ⁻¹)

Appendix B

TRANSMISSION-LINE FORMULAS

THIS PAGE INTENTIONALLY BLANK

Appendix B

TRANSMISSION-LINE FORMULAS

Quantity	General Line	Ideal Line	Approximate Results for Low-Loss Lines
Propagation constant $\gamma = \alpha + j\beta$	$\sqrt{(R + j\omega L)(G + j\omega C)}$	$j\omega\sqrt{LC}$	$(\alpha L \ll 1)$ (see α and β below)
Phase constant β	$\text{Im}(\gamma)$	$\omega\sqrt{LC} = \frac{\omega}{v} = \frac{2\pi}{\lambda}$	$\omega\sqrt{LC} \left[1 - \frac{RG}{4\omega^2 LC} + \frac{G^2}{8\omega^2 C^2} + \frac{R^2}{8\omega^2 L^2} \right]$
Attenuation constant α	$\text{Re}(\gamma)$	0	$\frac{R}{2Z_0} + \frac{GZ_0}{2}$
Characteristic impedance Z_0	$\sqrt{\frac{R + j\omega L}{G + j\omega C}}$	$\sqrt{\frac{L}{C}}$	$\sqrt{\frac{L}{C}} \left[1 + j \left(\frac{G}{2\omega C} - \frac{R}{2\omega L} \right) \right]$
Input impedance Z_i	$Z_0 \frac{Z_L \cosh \gamma l + Z_0 \sinh \gamma l}{Z_0 \cosh \gamma l + Z_L \sinh \gamma l}$ or $Z_0 \frac{1 + pe^{-2\gamma l}}{1 - pe^{-2\gamma l}}$	$Z_0 \frac{Z_L \cos \beta l + jZ_0 \sin \beta l}{Z_0 \cos \beta l + jZ_L \sin \beta l}$	$Z_0 \left[\frac{\alpha l \cos \beta l + j \sin \beta l}{\cos \beta l + j\alpha l \sin \beta l} \right]$
Impedance of shorted line	$Z_0 \tanh \gamma l$	$jZ_0 \tan \beta l$	$Z_0 \left[\frac{\alpha l \cos \beta l + j \sin \beta l}{\cos \beta l + j\alpha l \sin \beta l} \right]$

Appendix B

TRANSMISSION-LINE FORMULAS

Quantity	General Line	Ideal Line	Approximate Results for Low-Loss Lines
Propagation constant $\gamma = \alpha + j\beta$	$\sqrt{(R + j\omega L)(G + j\omega C)}$	$j\omega\sqrt{LC}$	$(\alpha L \ll 1)$ (see α and β below)
Phase constant β	$\text{Im}(\gamma)$	$\omega\sqrt{LC} = \frac{\omega}{v} = \frac{2\pi}{\lambda}$	$\omega\sqrt{LC} \left[1 - \frac{RG}{4\omega^2 LC} + \frac{G^2}{8\omega^2 C^2} + \frac{R^2}{8\omega^2 L^2} \right]$
Attenuation constant α	$\text{Re}(\gamma)$	0	$\frac{R}{2Z_0} + \frac{GZ_0}{2}$
Characteristic impedance Z_0	$\sqrt{\frac{R + j\omega L}{G + j\omega C}}$	$\sqrt{\frac{L}{C}}$	$\sqrt{\frac{L}{C}} \left[1 + j \left(\frac{G}{2\omega C} - \frac{R}{2\omega L} \right) \right]$
Input impedance Z_i	$Z_0 \left[\frac{Z_L \cosh \gamma l + Z_0 \sinh \gamma l}{Z_0 \cosh \gamma l + Z_L \sinh \gamma l} \right]$ or $Z_0 \frac{1 + pe^{-2\gamma l}}{1 - pe^{-2\gamma l}}$	$Z_0 \left[\frac{Z_L \cos \beta l + jZ_0 \sin \beta l}{Z_0 \cos \beta l + jZ_L \sin \beta l} \right]$	$Z_0 \left[\frac{\alpha l \cos \beta l + j \sin \beta l}{\cos \beta l + j\alpha l \sin \beta l} \right]$
Impedance of shorted line	$Z_0 \tanh \gamma l$	$jZ_0 \tan \beta l$	

Appendix B (Concluded)

Quantity	General Line	Ideal Line	Approximate Results for Low-Loss Lines
Impedance of open line	$Z_o \coth \gamma \ell$	$-jZ_o \cot \beta \ell$	$Z_o \left[\frac{\cos \beta \ell + j\alpha \ell \sin \beta \ell}{\alpha \ell \cos \beta \ell + j \sin \beta \ell} \right]$
Voltage along line $V(z)$	$V_i \cosh \gamma z - I_i Z_o \sinh \gamma z$ or $V_i(0)e^{-\gamma z} \frac{1 + \rho e^{2\gamma z}}{1 + \rho}$	$V_i \cos \beta z - jI_i Z_o \sin \beta z$	
Current along line $I(z)$	$I_i \cosh \gamma z - \frac{V_i}{Z_o} \sinh \gamma z$ or $I_i(0)e^{-\gamma z} \frac{1 - \rho e^{2\gamma z}}{1 - \rho}$	$I_i \cos \beta z - j \frac{V_i}{Z_o} \sin \beta z$	
Reflection coefficient P_R	$\frac{Z_L - Z_o}{Z_L + Z_o}$	$\frac{Z_L - Z_o}{Z_L + Z_o}$	

Notes: R, L, G, C = Distributed resistance, inductance, conductance, capacitance per unit length.

ℓ = Length of line.

Subscript i = Input end quantities.

Subscript L = Load end quantities.

z = Distance along line from input end.

λ = Wavelength measured along line.

v = Velocity of light in dielectric.

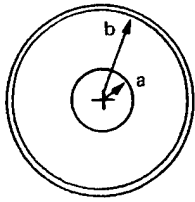
Appendix C

CHARACTERISTIC IMPEDANCE OF TRANSMISSION-LINE CONFIGURATIONS

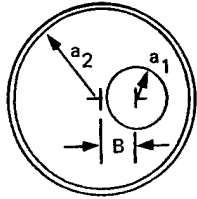
THIS PAGE INTENTIONALLY BLANK

Appendix C

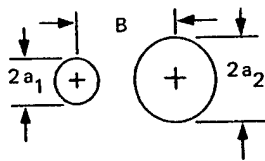
CHARACTERISTIC IMPEDANCE OF TRANSMISSION-LINE CONFIGURATIONS



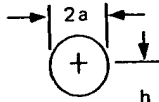
$$Z_o = \frac{\eta}{2\pi} \log \frac{b}{a}$$



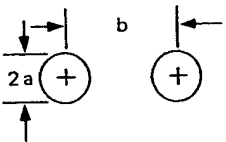
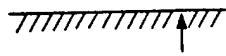
$$Z_o = \frac{\eta}{2\pi} \cosh^{-1} \left[\frac{a_1^2 + a_2^2 - B^2}{2a_1 a_2} \right]$$



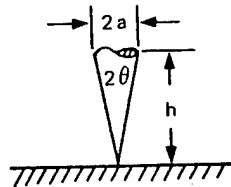
$$Z_o = \frac{\eta}{2\pi} \cosh^{-1} \left[\frac{B^2 - a_1^2 - a_2^2}{2a_1 a_2} \right]$$



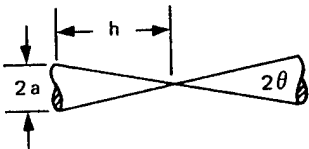
$$Z_o = \frac{\eta}{2\pi} \cosh^{-1} \frac{h}{a} \approx \frac{\eta}{2\pi} \log \frac{2h}{a} \quad \left(\frac{h}{a} \gg 1 \right)$$



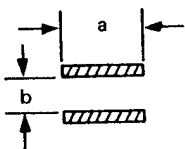
$$Z_o = \frac{\eta}{\pi} \cosh^{-1} \frac{b}{2a} \approx \frac{\eta}{\pi} \log \frac{b}{a} \quad \left(\frac{b}{a} \gg 1 \right)$$



$$Z_o = \frac{\eta}{2\pi} \log \cot \frac{\theta}{2} \approx \frac{\eta}{2\pi} \log \frac{2h}{a} \quad (\theta \ll 1)$$



$$Z_o = \frac{\eta}{\pi} \log \cot \frac{\theta}{2} \approx \frac{\eta}{\pi} \log \frac{2h}{a} \quad (\theta \ll 1)$$



$$Z_o = \eta \frac{b}{a} \quad (a \gg b)$$

$$\eta = \sqrt{\frac{\mu}{\epsilon}}$$

$$v = \frac{1}{\sqrt{\mu\epsilon}}$$

$$Z_o = \sqrt{\frac{L}{C}}$$

$$C = \frac{1}{vZ_o}$$

$$L = \frac{Z_o}{v}$$

$$\cosh^{-1} \frac{h}{a} \approx \log \frac{2h}{a} \quad (h \gg a)$$

THIS PAGE INTENTIONALLY BLANK

Appendix D

CONDUCTIVITY AND RELATIVE PERMEABILITY
OF SHIELDING MATERIALS

THIS PAGE INTENTIONALLY BLANK

Appendix D

CONDUCTIVITY AND RELATIVE PERMEABILITY
OF SHIELDING MATERIALS

Material	Conductivity, σ (mho/m)	Relative Permeability, μ_r
Silver	6.8×10^7	1
Copper	5.8×10^7	1
Brass	1.4×10^7	1
Aluminum	3.7×10^7	1
Lead	4.5×10^6	1
Nickel	1.3×10^7	100
Mild steel	6×10^6	500
High- μ Alloy	1.6×10^6	5×10^4

THIS PAGE INTENTIONALLY BLANK

Appendix E

WIRE TABLE

THIS PAGE INTENTIONALLY BLANK

Appendix E

WIRE TABLE

Solid Copper			Resistance				Weight (pounds/ 1000 ft) 20° C
			Standard Annealed-- 100% Conductivity			Hard- Drawn†	
AWG or B & S	Diameter (mils)	Area (circular mils)	Ohms/1000 ft*			20° C	
			0° C	20° C	50° C		
0000	460.0	211,600	0.0451	0.0490	0.0548	0.0504	640.5
000	409.6	167,806	0.0569	0.0618	0.0691	0.0635	507.9
00	364.8	133,077	0.0717	0.0779	0.0871	0.0801	402.8
0	324.9	105,535	0.0906	0.0983	0.1099	0.1010	319.5
1	289.3	83,693	0.1141	0.1239	0.1385	0.1273	253.3
2	257.6	66,371	0.1440	0.1563	0.1748	0.1606	200.9
3	229.4	52,635	0.1815	0.1970	0.2203	0.2025	159.3
4	204.3	41,741	0.2289	0.2485	0.2778	0.2554	126.4
5	181.9	33,102	0.2886	0.3133	0.3503	0.3220	100.2
6	162.0	26,251	0.3640	0.3951	0.4418	0.4061	79.46
7	144.3	20,818	0.4590	0.4982	0.5570	0.5120	63.02
8	128.5	16,510	0.5787	0.6282	0.7024	0.6456	49.98
9	114.4	13,093	0.7297	0.7921	0.8856	0.8141	39.63
10	101.9	10,383	0.9203	0.9989	1.117	1.027	31.43
11	90.74	8,234	1.161	1.260	1.409	1.295	24.92
12	80.81	6,530	1.463	1.588	1.775	1.632	19.77
13	71.96	5,178	1.845	2.003	2.240	2.059	15.68
14	64.08	4,107	2.326	2.525	2.823	2.595	12.43
15	57.07	3,257	2.933	3.184	3.560	3.272	9.858
16	50.82	2,583	3.700	4.016	4.490	4.127	7.818
17	45.26	2,048	4.665	5.064	5.662	5.204	6.200
18	40.30	1,624	5.882	6.385	7.139	6.562	4.917
19	35.89	1,288	7.418	8.051	9.002	8.274	3.899
20	31.96	1,022	9.351	10.15	11.35	10.43	3.092

Appendix E (Concluded)

Solid Copper			Resistance				Weight (pounds/ 1000 ft) 20° C
			Standard Annealed-- 100% Conductivity			Hard- Drawn [†]	
AWG or B & S	Diameter (mils)	Area (circular mils)	Ohms/1000 ft*			20° C	
			0° C	20° C	50° C		
21	28.46	810.1	11.79	12.80	14.31	13.16	2.452
22	25.35	642.4	14.87	16.14	18.05	16.59	1.945
23	22.57	509.5	18.76	20.36	22.76	20.92	1.542
24	20.10	404.0	23.65	25.67	28.70	26.38	1.223
25	17.90	320.4	29.82	32.37	36.19	33.27	0.9699
26	15.94	254.1	37.60	40.81	45.63	41.94	0.7692
27	14.20	201.5	47.42	51.47	57.55	52.90	0.6100
28	12.64	159.8	59.80	64.90	72.57	66.70	0.4837
29	11.26	126.7	75.39	81.83	91.49	84.10	0.3836
30	10.03	100.5	95.07	103.2	115.4	106.1	0.3042
31	8.928	79.70	119.9	130.1	145.5	133.7	0.2413
32	7.950	63.21	151.2	164.1	183.5	168.6	0.1913
33	7.080	50.13	190.6	206.9	231.3	212.6	0.1517
34	6.305	39.75	240.4	260.9	291.7	268.1	0.1203
35	5.615	31.52	303.1	329.0	367.9	338.1	0.09542
36	5.000	25.00	382.1	414.8	463.8	426.3	0.07568
37	4.453	19.83	481.9	523.1	584.9	537.6	0.06001
38	3.965	15.72	607.7	659.6	737.5	677.9	0.04759
39	3.531	12.47	766.3	831.8	930.0	854.9	0.03774
40	3.145	9.89	966.4	1049	1173	1078	0.02993

* Resistance at the stated temperature of a wire whose length is 1000 ft at 20° C.

† 97.3% conductivity.

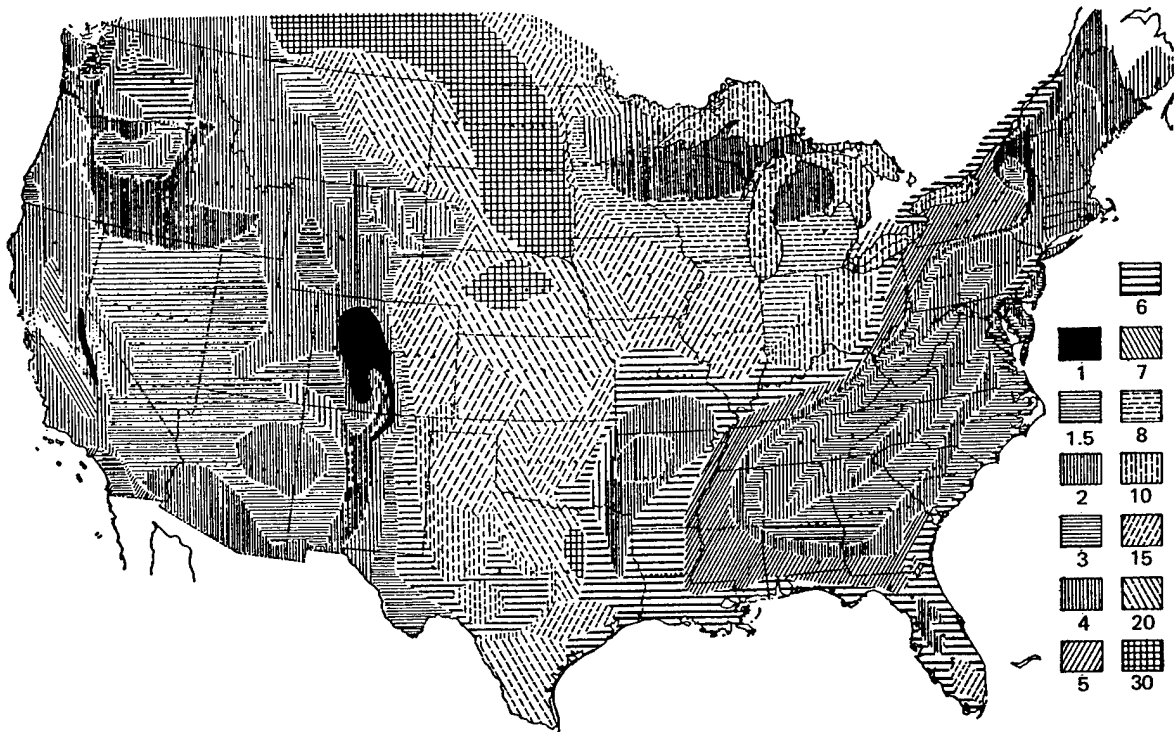
Appendix F

GROUND CONDUCTIVITY IN THE UNITED STATES

THIS PAGE INTENTIONALLY BLANK

Appendix F

GROUND CONDUCTIVITY IN THE UNITED STATES*



* Numbers on the legend, when multiplied by 10^{-3} , indicate ground conductivity in mhos/meter. (Map by FCC.)